

# We are IntechOpen, the world's leading publisher of Open Access books Built by scientists, for scientists

6,900

Open access books available

186,000

International authors and editors

200M

Downloads

Our authors are among the

154

Countries delivered to

TOP 1%

most cited scientists

12.2%

Contributors from top 500 universities



WEB OF SCIENCE™

Selection of our books indexed in the Book Citation Index  
in Web of Science™ Core Collection (BKCI)

Interested in publishing with us?  
Contact [book.department@intechopen.com](mailto:book.department@intechopen.com)

Numbers displayed above are based on latest data collected.  
For more information visit [www.intechopen.com](http://www.intechopen.com)



# Geosynthetic Reinforced Embankment Slopes

*Akshay Kumar Jha and Madhav Madhira*

## Abstract

Slope failures lead to loss of life and damage to property. Slope instability of natural slope depends on natural and manmade factors such as excessive rainfall, earthquakes, deforestation, unplanned construction activity, etc. Manmade slopes are formed for embankments and cuttings. Steepening of slopes for construction of rail/road embankments or for widening of existing roads is a necessity for development. Use of geosynthetics for steep slope construction considering design and environmental aspects could be a viable alternative to these issues. Methods developed for unreinforced slopes have been extended to analyze geosynthetic reinforced slopes accounting for the presence of reinforcement. Designing geosynthetic reinforced slope with minimum length of geosynthetics leads to economy. This chapter presents review of literature and design methodologies available for reinforced slopes with granular and marginal backfills. Optimization of reinforcement length from face end of the slope and slope - reinforcement interactions are also presented.

**Keywords:** slopes, geosynthetics, reinforcement, optimization of length, marginal soils, steepening

## 1. Introduction

Landslides in slopes and failures of embankment and cut slopes lead to loss of life and property. Several factors, natural and manmade, such as heavy rainfall, unplanned construction, deforestation, restricting waterways of rivers and their tributaries are major causes for instability of slopes. Factors controlling stability of natural slopes are type of soil, environmental conditions, groundwater, stress history, rainfall, cloud burst, earthquakes, etc. Landslide mortality rate exceeds one per 100 km<sup>2</sup> per year in developing countries like India, China, Nepal, Peru, Venezuela, Philippines and Tajikistan [1, 2]. Factors that cause man-made slope failure are very different and could be due to inadequate design, improper backfill, poor construction, etc. The repair of failed slope involves removal of debris and reinstatement of slope with free draining material. Restoration of the slide with geosynthetics can be simpler, faster and economical. Designing slopes with Geosynthetics has several advantages (Simac [3]), e.g., reduced land requirement, additional usable area at toe of slope, use of available on-site soil, reduced transportation costs of select fill or export costs of unsuitable fill, steeper slopes, elimination of concrete facing, and facilitation of natural vegetation for sustainable development.

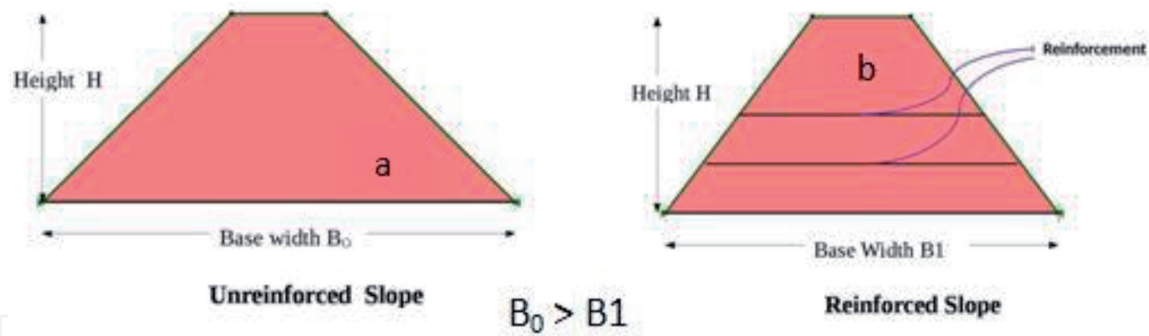


**Figure 1.** Effect of geosynthetic reinforcement on geometry of embankment: (a) flat and (b) steep slopes.

Embankments are built with engineered fills. Geosynthetics facilitate reduction of earthwork volume by altering the geometry of the embankment (**Figure 1**) and even allow use of marginal soil.

In reinforced soil, conventionally free draining material is specified for backfill due to its high strength and draining properties. The cost of fill material is about 40% of the total cost of the structure [4]. If marginal soil is used instead it could be more economical. Apart from economics, technical factors like esthetics, reliability, simple construction techniques, good seismic performance and ability to tolerate large deformations without structural distress have enhanced the acceptance and use of geosynthetics as reinforcing material.

## 2. Case histories

### 2.1 Tallest geosynthetic reinforced slope

One of the tallest geogrid reinforced green faced slope 1H:1 V and 74 m high (**Figure 2**) is airport runway extension in Charleston, West Virginia [5]. **Figure 3** depicts a schematic of the reinforced slope.

The high angle of shearing resistance of  $36^\circ$  of onsite soils provided two significant benefits viz., no need to import borrow soil and minimum required embedment length. However, there was a partial failure of this slope which was restored subsequently.

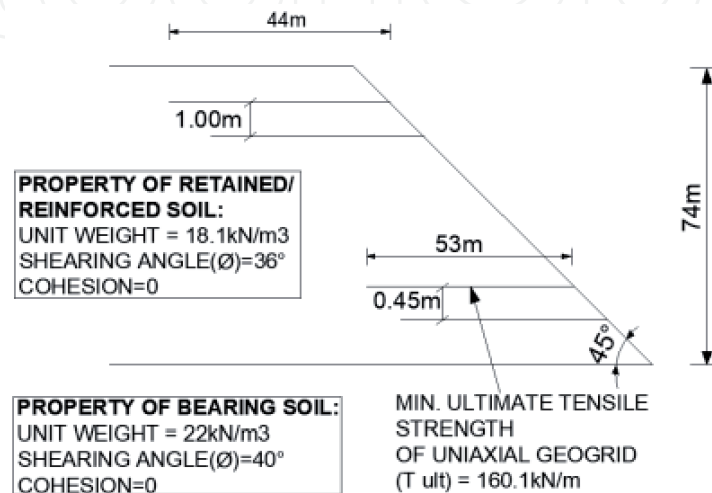


**Figure 2.** Schematic of reinforced embankment for Yeager runway extension (redrawn based on [5]).



**Figure 3.**  
 Reinforced slope Yeager runway extension (after [5]).

## 2.2 Geogrid reinforced embankment with steep side slopes

For a highway project in Brampton, Ontario, property acquisition costs and other problems necessitated the design of 7 m high embankment with 1H:1 V steep side slopes. Cost-benefit studies showed that steep side slopes reinforced with synthetic tensile elements were considerably cheaper than the other alternatives. Design and construction of 7 m high embankment with slopes using geogrids (**Figure 4**) as an alternative to rock fill embankment with side slopes of 1.25H:1 V requiring additional land has been covered by Devata [6]. Reinforced earth slope was found to be most economical (**Table 1**). The total cost of 1H:1 V reinforced slope is the least among all the alternatives making it the most economical option.

## 2.3 Composite soil reinforcement system for very high and steep fills for Sikkim airport

For runway construction of airport at Pakyong in north eastern Indian state of Sikkim huge cutting of earth and its filling on the valley side was required to form a level platform to provide runway of 1820 m x 150 m and other related

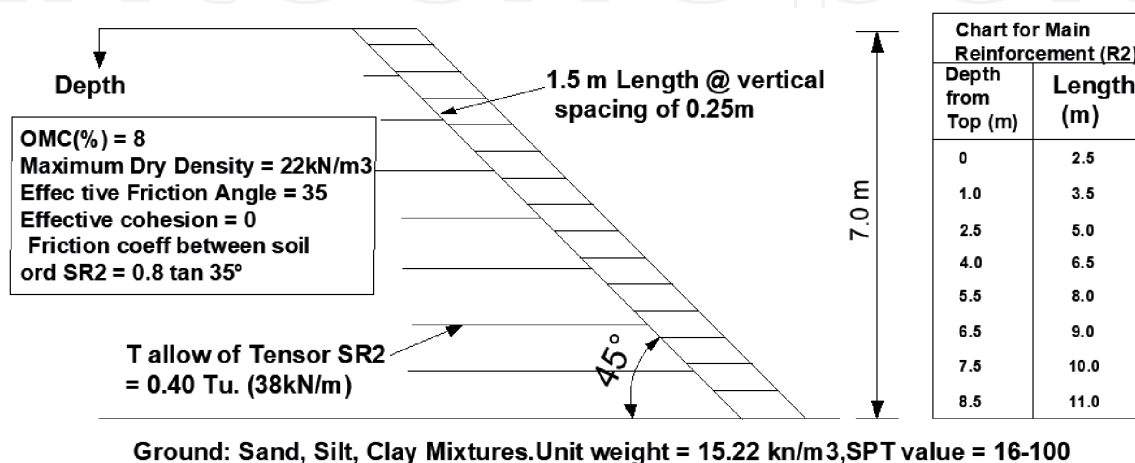


**Figure 4.**  
 Schematic of reinforced slope for highway extension (sketch based on [6]).

Construction Method	Construction cost \$M	Property Cost \$M	Total Cost \$M
Reinf. Concrete Wall	1.52	Nil	1.52
Reinforced Earth Wall	1.42	Nil	1.42
1.25H:1 V Rockfill	0.93	0.30	1.23
1H:1 V Reinf. Slope	0.48	Nil	0.48
2H:1 V Earth Fill	0.30	0.90	1.20

**Table 1.**  
*Cost comparison of different options.*

infrastructures over 200-acre area. Retention of fill on the valley side needed construction of retaining structures with heights varying from 30 to 74 m over a length of 1480 m (**Figure 5**).

On hill side, the cut slopes have a height extending up to 100 m. To retain and stabilize this fill of varying height, a composite soil reinforcement system was employed [7]. To make optimum utilization of space available and minimize cost, combination of vertical wall and steep slope has been adopted for construction of retaining structure. Facing elements for the reinforced soil wall comprise of Gabions (**Figure 6**).



**Figure 5.**  
*Sikkim airport - aerial view (after [7]).*



**Figure 6.**  
*Slope face completely covered with vegetation few months after installation (after [7]).*

### 3. Geosynthetics

Geosynthetics are mostly planar products manufactured from polymeric material and used with geomaterials such as soil and rock, as integral part of manmade project or system for better performance, economy, better quality control, rapid installation, cost competitiveness, lower carbon footprint, requirement of smaller parcel of land for embankments, etc.

Geotextiles and Geogrids are used normally for reinforcing embankments or natural slopes either to obtain higher factor of safety or for construction with steep slopes. Allowable Geotextile/Geogrid strength is arrived at using several factors to account for degradation, creep, installation damage, etc. The allowable tensile strength,  $T_{all}$ , is

$$T_{all} = T_{ult} / R_{FID} * R_{FCR} * R_{FCBD} \quad (1)$$

Where  $T_{all}$  and  $T_{ult}$  - allowable and ultimate tensile strengths respectively,  $R_{FID}$ ,  $R_{FCR}$  and  $R_{FCBD}$  - reduction factors (all >1.0) for installation, creep and chemical and biological damage respectively. The combined or overall reduction factor is about 2.0 for design.

### 4. Literature review

Jewell et al. [8], Bonaparte et al. [9] and Verduin and Holtz [10] present design methods for earth slopes reinforced with geotextiles and/or geogrids using limit equilibrium method considering circular or/and bilinear wedges. Leshchinsky and Reinschmidt [11] and Leshchinsky and Boedeker [12] present an approach based on limit equilibrium and variational extremization of factor of safety of multilayer reinforced slope. Schneider and Holtz [13] present a design procedure for slopes reinforced with geotextiles and geogrids for a bilinear surface of sliding, considering porewater pressures and the initial stress conditions in the slope. Jewell [14] presented revised design charts for steep slopes valid for all reinforcement materials. Leshchinsky [15] and Leshchinsky et al. [16] used log-spiral failure mechanism to determine the required reinforcement long term strength. Zhao [17] and Michalowski [18] present kinematic limit analyses solutions for the stability of reinforced soil slopes. Shiwakoti et al. [19] conducted parametric studies to investigate the effect of geosynthetic strength, soil-geosynthetic interaction coefficients, vertical spacing of geosynthetics for soil slope/wall on competent foundation. Baker and Klein [20, 21] modified the top-down approach of Leshchinsky [15] to obtain the reinforcement force needed for a prescribed factor of safety everywhere within the reinforced mass. Han and Leshchinsky [22] present a general analytical framework for design of flexible reinforced earth structures, i.e., walls and slopes. Leshchinsky et al. [23] present a limit equilibrium methodology to determine the unfactored global geosynthetic strength required to ensure sufficient internal stability in reinforced earth structures. Leshchinsky et al. [24] introduced a limit state design framework for geosynthetic reinforced slopes and walls. Leshchinsky and Ambauen [25] present use of upper bound limit analysis (LA) in conjunction with discretization procedure known as discontinuity layout optimization (DLO). DLO-LA is an effective tool for establishing a critical failure mechanism and ensuing stability of the slope without the constraint or assumptions required in LE analysis. Shukla et al. [26] presented a review of design of reinforced slope and covers basic of methods in detail. Gao et al. [27] in their study considered three-dimensional effect on reinforced earth structure stability and to determine the required

strength and length of reinforcement using limit analysis. Song et al. [28] proposed new approach based on LE principle to evaluate stability of reinforced slope.

Free draining granular material is used conventionally for reinforced earth slope construction. However cohesive materials have also been used for construction of reinforced slopes in few cases. Very few design guidelines/methods are available for design of reinforced earth slope with marginal soil. Christopher et al. [29] provide design guidance (total stress analysis ignoring the drainage contribution of geocomposite for short term and effective stress analysis considering drainage in the long term) for reinforced soil structures using poorly draining backfills. Naughton et al. [30] improved the design method of Christopher et al. [29] and presented single stage effective stress analysis since excess pore pressure gets dissipated fully before construction of subsequent layers. Clancy and Naughton [31] used design approach of Naughton et al. [30] to design four steep slopes using fine-grained soils as backfill material and provided a method to determine the maximum height of each lift to allow dissipation of excess pore pressures in a 24-hour period for a 10 m high 70° slope. Giroud et al. [32] updated design method of Naughton et al. [30] for reinforced slopes and walls using draining geogrid, with focus on improved determination of the required transmissivity of the same. Naughton et al. [33] conducted a parametric study of design parameters of low permeability fill and concluded that for typical compressibility and consolidation parameters vertical spacing of the reinforcement of 0.5 m is adequate.

Abd and Utili [33] employed limit analysis approach and semi-analytical method for uniform slopes that provide the amount of reinforcement needed as a function of cohesion,  $c$ , and angle of shearing resistance,  $\phi$ , of backfill, tensile strength of geosynthetic and of the slope inclination.

## **5. Design methods**

Geosynthetic reinforced slopes are designed to provide internal, external, global and surfacial stability. Surfacial stability determines the requirement of secondary reinforcement to ensure no shallow sloughing. The design process must address all possible failure modes that a reinforced (or unreinforced) slope would potentially experience. The design addresses internal stability (pull out and bond failures) for the condition where the failure surface intersects the reinforcement, external stability (sliding, overturning, bearing failures) for the condition where the failure surface is located outside and below the reinforced soil mass and compound stability for the condition where the failure plane passes behind and through the reinforced soil mass. In order to analyze a reinforced slope the requirements include the slope geometry, external and seismic loading, porewater pressure and/or seepage conditions, soil parameters and properties, the reinforcement parameters and properties, the interaction characteristics of the soil and the geosynthetic. The design of a reinforced soil slope determines the final geometry, the required number, spacing and lengths of reinforcement layers and measures to prevent sloughing or erosion of the slope face.

Methods originally developed for unreinforced slopes have been extended to reinforced slopes accounting for the presence of reinforcement. Methods available for analyzing geosynthetic reinforced soil slopes are (i) Limit equilibrium, (ii) Limit analysis, (iii) Slip line and (iv) Finite element methods.

### **5.1 Limit equilibrium method**

Conventional geotechnical engineering approach to slope stability problems is to use limit equilibrium concepts on an assumed circular or non-circular failure

surface and to arrive at a factor of safety. Factor of safety is estimated using moment and/or force equilibrium equations considering the reinforcing effect of geosynthetics. Several limit equilibrium methods have been used in various studies [34–39].

## 5.2 Limit analysis

Limit analysis is another method for solution of slope stability problems [17, 19, 25, 40–44]. It is based on plasticity theory and can be applied to slopes of arbitrary geometry and complex loading conditions. Using limit theorems, collapse load can be bracketed between lower and upper bounds even if it cannot be determined exactly. Recent approaches that combine finite elements and failure criterion have narrowed the gap between the two bounds.

## 5.3 Slip line method

Slip line method is based on stress characteristics and based on homogenization of the composite mass and suitable for continuous filament or fiber reinforced soil slopes. Failure criterion for geosynthetic reinforced soil composite was presented by Michalowski and Zhao [40]. Limit loads on geosynthetic reinforced soil slopes using slip line method were given by Zhao [17].

## 5.4 Finite element method

Finite element method of analysis is generally based on quasi-elastic continuum mechanics approach in which stresses and strains are estimated throughout the mass. In this method both deformation and strength parameters, viz., modulus of deformation ( $E$ ), Poisson's ratio ( $\nu$ ), cohesion,  $c$ , angle of shearing resistance,  $\phi$ , angle of dilation ( $\psi$ ) are required for design. Alternately, shear strength reduction technique is used for design of slope considering the effect of reinforcement. In this approach no assumption needs to be made regarding nature of failure surface or its location as failure occurs “naturally” through the zones within the soil mass wherein the shear stresses attain values close to the strength of the soil. Details of this approach can be found in the works of Rowe and Soderman [45], Almeida et al. [46], Chalaturnyk et al. [47], Ali and Tee [48] and Griffith and Lane [49]. Software such as Plaxis, FLAC, etc., are available for the analysis by ‘Soil Strength Reduction Technique’ using FEM.

# 6. Reinforced embankment slope design - Jewell method

## 6.1 Jewell et al. design method

Jewell et al. [8] proposed a method of design based on Limit Equilibrium analysis and local check on individual reinforcement spacing for geogrid reinforced embankment slope for slope angles,  $\beta$ , ranging from  $30^\circ$  to  $80^\circ$ . Embankment soil is granular and the crest is horizontal. Length of reinforcement is based on (i) no overstressing of lower layers, (ii) no outward sliding along the interface between soil and reinforcement layer and (iii) no tension on the base. Two-part wedge analysis is used and critical wedge surface for failure is located by varying wedge angles  $\theta_1$  and  $\theta_2$  (**Figure 7**) and the location of intersection of the two wedge lines, i.e., the wedge point.

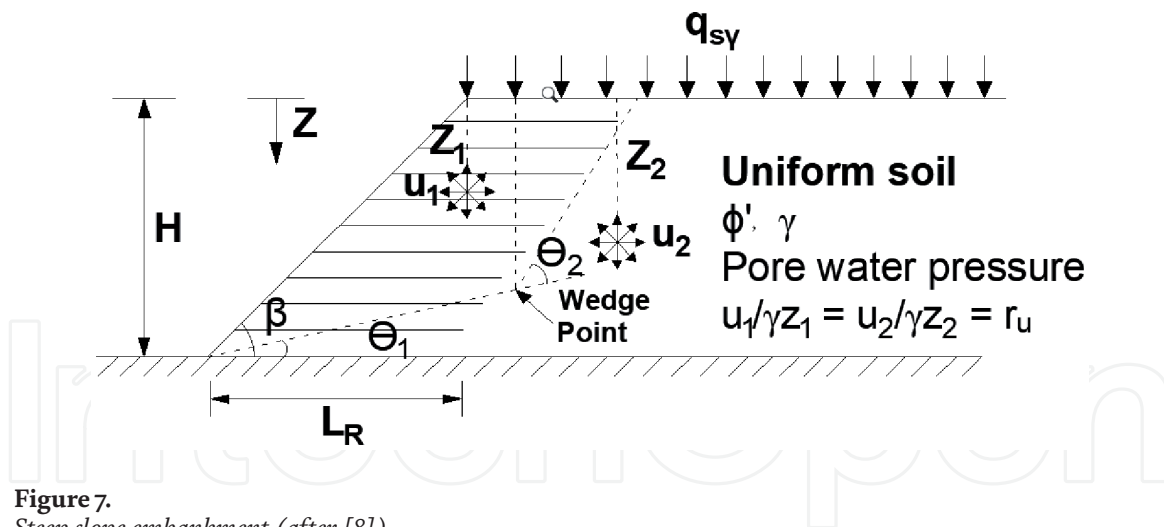


**Figure 7.**  
Steep slope embankment (after [8]).

The interslice forces are assumed to be zero. Design charts calculate total reinforcement force and length of reinforcement in terms of slope angle,  $\beta$ , effective critical state friction angle of soil,  $\phi_c$ , and porewater pressure parameter,  $r_u = u / \gamma z$ . The strength of reinforcement is the strength of geogrid at the end of design life for most severe condition expected during service life. Factor of safety of 1.3 to 1.5 for the slope is achieved by applying the same to the reinforcement strength as well. All reinforcement layers are of equal length. Surcharge and earthquake loads are not included in the analysis.

## 6.2 Revised design

Jewell [14] revised the previous design for geotextiles and geogrids as reinforcement. Interaction between soil and horizontal reinforcement has been considered in terms of bond coefficient ( $f_b$ ) which governs the load transfer between reinforcement and soil. The basic philosophy of design is that available stress from the reinforcement exceeds the required stress for equilibrium in soil. Improvements over previous design method are given in **Table 2**.

### 6.2.1 Design parameters for soil and reinforcement

Allowable Tensile Strength ( $T_{all}$ ) for reinforcement is chosen such that strain in reinforcement does not exceed 3–5% during design life to ensure satisfactory serviceability.  $\phi_d = \phi_c$ . Porewater pressure to be considered should include the worst condition expected in design life. Design values of  $\phi_d$ ,  $r_u$ ,  $\beta$  and  $H$  are used to

SN	Parameter	Jewell et al. [8]	Jewell [14]
1	Slope angle ( $\beta$ )	$80^\circ \leq \beta \leq 30^\circ$	$90^\circ \leq \beta \leq 30^\circ$
2	Bond coefficient ( $f_b$ )	Reinforcement bond angle of friction = 50% design friction angle of soil	$1 \geq f_b \geq 0$
3	Direct Sliding coefficient ( $f_{ds}$ )	Friction resistance to direct sliding = 80% design friction angle of soil	$f_{ds} = 0.80$ and correction factor applied whenever $f_{ds}$ takes a value less than 0.8.
4	Reinforcing material	Geogrid	Geogrid and Geotextile

**Table 2.**  
Salient improvements over Jewell et al. [14].

determine required earth pressure coefficient,  $K_{req}$ , and reinforcement length,  $L_R/H$ , from the design charts. Design charts for  $r_u = 0, 0.25$  and  $0.50$  are shown in **Figures 8** and **9**. Large strain or critical state shearing resistance ( $\phi_c$ ) of soil is to be used for design.

### 6.3 Limit equilibrium (LE) method of stability analysis

Various LE Methods such as Bishop's Simplified, Janbu's Simplified, Spencer, Morgenstern-Price, Janbu Generalized, Sarma, etc., have been developed for slope stability analysis. The problem is considered in two dimension i.e. plane strain case. The primary difference among all these methods lies in the equations of statics considered, which interslice normal and shear forces are included, and the assumed relationship between the interslice forces. **Tables 3** and **4** summarize the conditions for some of the common methods of stability analysis.

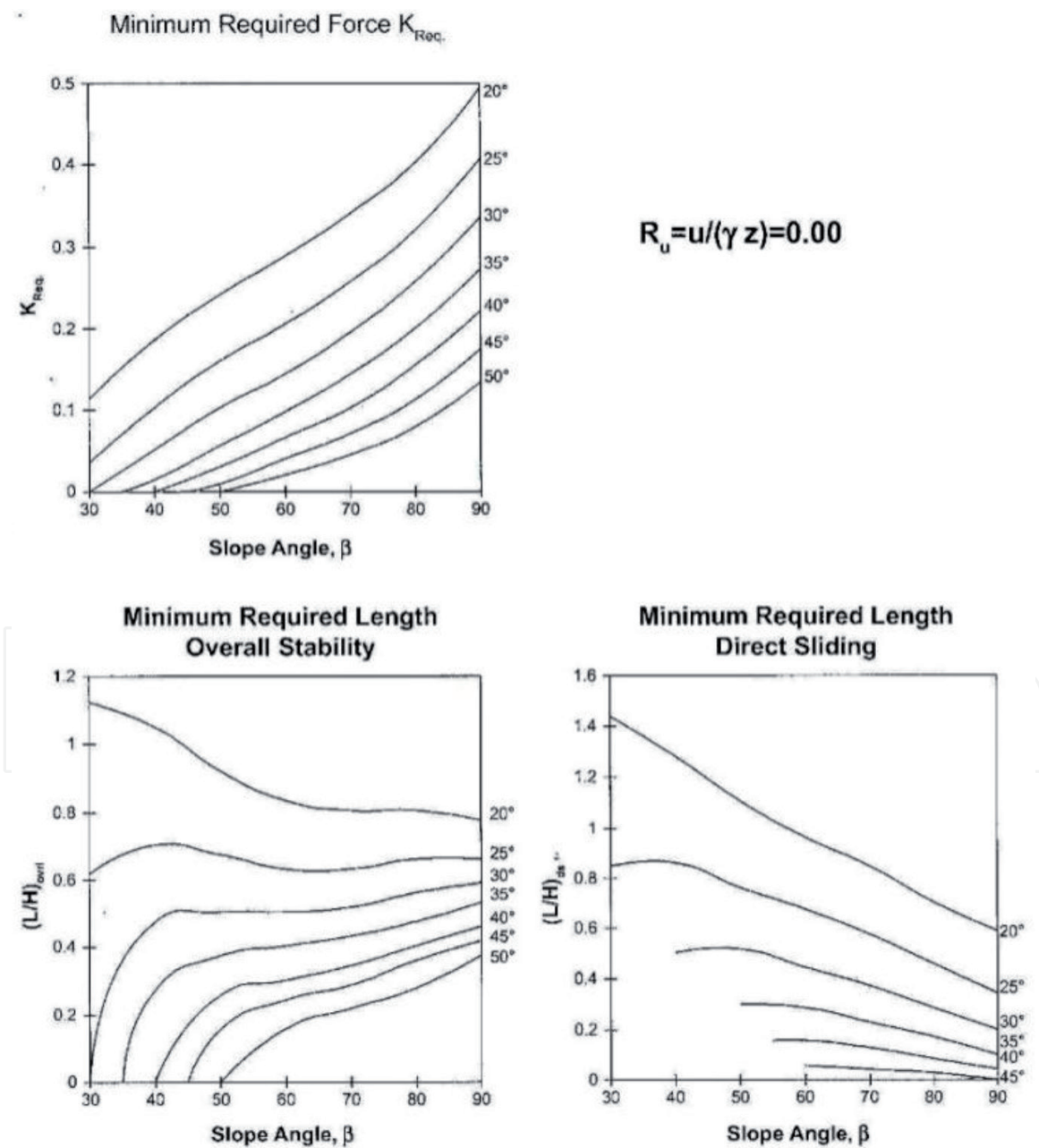


**Figure 8.**  
 Design chart for  $r_u = 0$  after Jewell [14].

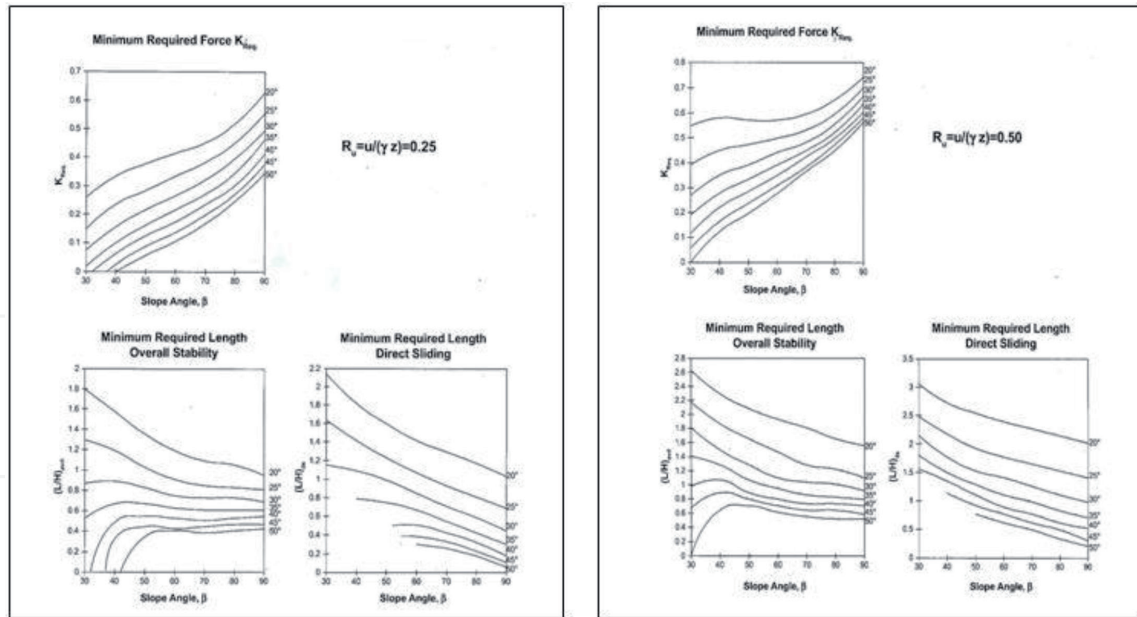


**Figure 9.**  
Design charts for  $r_u = 0.25$  and  $0.5$  after Jewell [14].

Method	Moment Equilibrium	Force Equilibrium
Ordinary or Fellenius	Yes	No
Bishop's Simplified	Yes	No
Janbu's Simplified	No	Yes
Spencer	Yes	Yes
Morgenstern-Price	Yes	Yes
Janbu Generalized	Yes (by slice)	Yes
Sarma – vertical slices	Yes	Yes

**Table 3.**  
Equations of statics satisfied (after Krahn [50]).

Method	Interslice Normal (E)	Interslice Shear (X)	Inclination of X/E Resultant, and X-E Relationship
Ordinary or Fellenius	No	No	No interslice forces considered
Bishop's Simplified	Yes	No	Horizontal
Janbu's Simplified	Yes	No	Horizontal
Spencer	Yes	Yes	Constant
Morgenstern – Price	Yes	Yes	Variable; user function
Janbu Generalized	Yes	Yes	Applied line of thrust and moment equilibrium of slice
Sarma – vertical slices	Yes	Yes	$X = C + E \tan \phi$

**Table 4.**  
Interslice forces and relationships (after Krahn [50]).

### 6.3.1 Koerner's design method

Koerner [51] proposed a method of slices for analysis of geosynthetic reinforced homogeneous slope neglecting interslice forces. Assuming circular arc failure surfaces minimum FS is found by varying the radius and coordinates of the origin of the circle. For slope reinforced with horizontal layers (Figure 10) of geosynthetics, FS, is

$$FS = \frac{\sum_{i=1}^{i=n} (N_i \tan \phi + c \Delta l_i) R + \sum_{j=1}^{j=m} T_j Y_j}{\sum_{i=1}^{i=n} (w_i \sin \theta_i) R} \quad (2)$$

where  $W_i$  = weight of  $i^{\text{th}}$  slice,  $\theta_i$  = angle made by tangent to the failure arc at the center of  $i^{\text{th}}$  slice with the horizontal,  $N_i = W_i \cos \theta_i$ ,  $\Delta l_i$  = arc length of  $i^{\text{th}}$  slice,  $R$  = radius of circular curve,  $c$  and  $\phi$  - strength parameters,  $T_j$  = allowable tensile strength of geosynthetic at  $j^{\text{th}}$  layer,  $y_j$  = moment arm for  $j^{\text{th}}$  layer,  $m$  = number of geosynthetic layers,  $n$  = number of slices. For fine grained soil, the equation for FS simplifies to

$$FS = \frac{c L_{arc} R + \sum_{i=1}^m T_i Y_i}{WX} \quad (3)$$

where  $W$  = weight of circular slice and  $X$  is the horizontal distance of CG of soil mass from the center of the critical slip circle.

### 6.3.2 Generalized limit equilibrium method

A generalized limit equilibrium (GLE) formulation was developed by Fredlund and Krahn [52] and Fredlund et al. [53]. This method encompasses the key elements of all the methods listed in Table 2. The interslice shear forces (Morgenstern and Price [49]) are

$$X = E \lambda f(x) \quad (4)$$

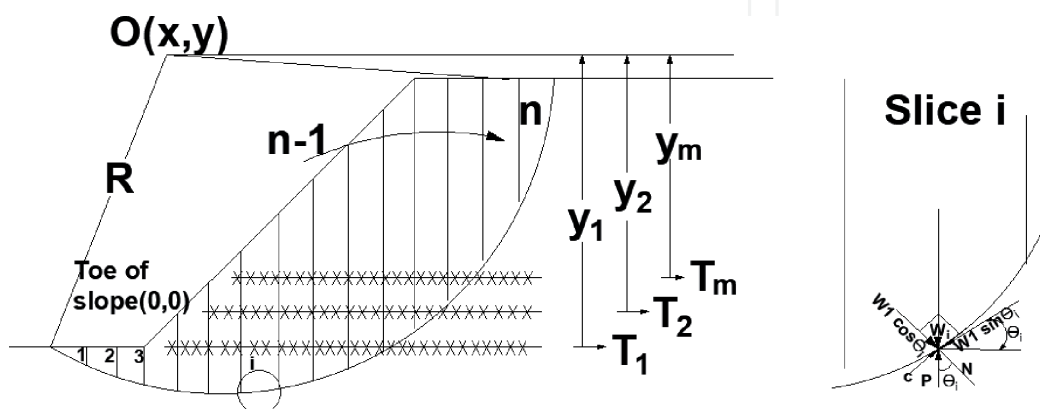


Figure 10. Circular arc slope stability analysis for geosynthetic reinforced  $c - \phi$  soil (after [44]).

Where  $f(x)$  –a function,  $E$  and  $X$  –the interslice normal force and shear forces respectively and  $\lambda$ - function. GLE Method showing forces on slice and geometrical parameters is shown in **Figure 11**.

The factor of safety,  $F_m$ , with respect to moment equilibrium is

$$F_m = \frac{\sum [C' \beta R + (N - u \beta) R \tan \phi']}{\sum Wx - \sum Nf \pm \sum Dd} \quad (5)$$

The factor of safety,  $F_f$ , with respect to horizontal force equilibrium is

$$F_f = \frac{\sum [C' \beta \cos \alpha + (N - u \beta) \tan \phi' \cos \alpha]}{\sum N \sin \alpha - D \cos \alpha} \quad (6)$$

where  $c'$  –effective cohesion,  $\phi'$ -effective angle of friction,  $u$  –pore water pressure,  $N$  –normal force on slice base,  $W$ –slice weight,  $D$ –line load and  $\beta$ ,  $R$ ,  $x$ ,  $f$ , and  $d$  – geometric parameters as detailed in **Figure 11**, and  $\alpha$  - inclination of slice base. One of the key variables in both the equations is  $N$  –the normal force at the base of each slice.  $N$  is obtained by the summation of vertical forces as

$$N = \frac{W + (XR - XL) - \frac{C' \beta \sin \alpha + u \beta \sin \alpha \tan \phi'}{F}}{\cos \alpha + \frac{\sin \alpha \tan \phi'}{F}} \quad (7)$$

The base normal force,  $N$ , is dependent on the interslice shear forces respectively  $XL$  and  $XR$  on the left and the right sides of the slice. The reinforcement force is accounted for in the analysis by GLE method.

### 6.3.3 Finite element computed stress in limit equilibrium

Krahn [45] suggested that normal stress determined from finite element stress analysis can be fed into General Limit Equilibrium Analysis. Thus, Limit Equilibrium and Finite Element method are integrated.

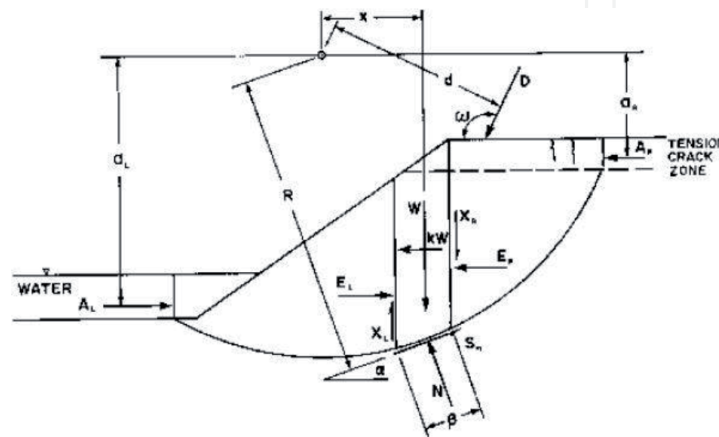


**Figure 11.** Forces acting on sliding mass with circular slip surface (after [47]).

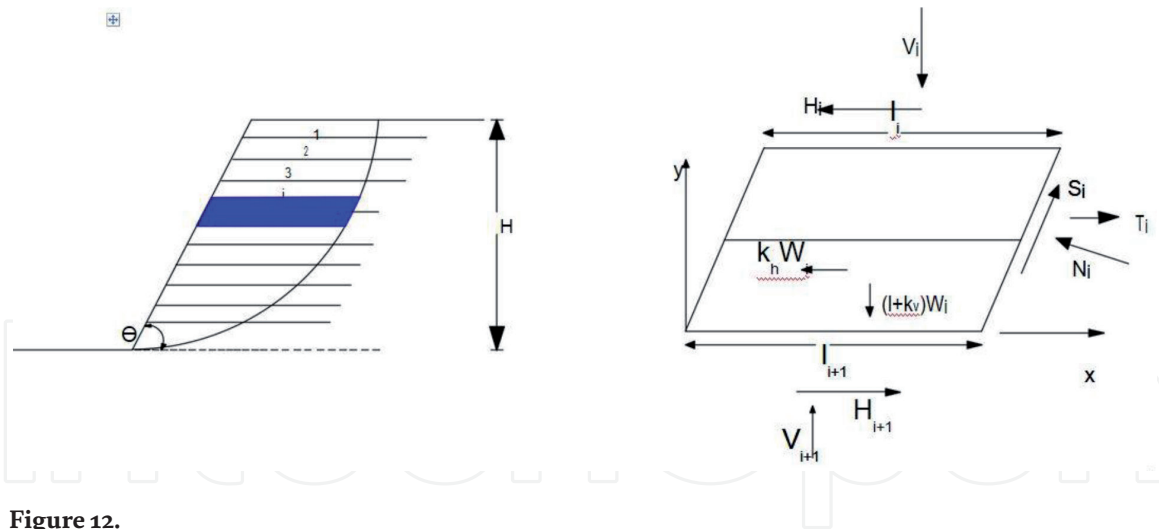


**Figure 12.**  
 Horizontal slice method (after Shahgholi and Fakher [39]).

### 6.3.4 Iterative GLE method for reinforced slope

Song et al. [28] proposed new approach based on LE principle to evaluate stability of reinforced slope. The effect of reinforcement is included as equivalent resisting force acting at slice base and added to GLE method. The corresponding equations are derived based on force equilibrium in the directions normal and parallel to slice base and moment equilibrium at the center of base of slice. The indeterminacy is resolved by assuming half sine function for inclination of inter-slice force in Eq. 4. The method satisfies both the force and the moment equilibrium considerations applicable to arbitrary failure surfaces and is iterative.

### 6.3.5 Horizontal slice method

Shahgholi and Fakher [39] proposed horizontal slice method (HSM) in which horizontal slices are used in place of vertical ones to analyze the stability of reinforced and unreinforced slopes and walls. The limitation of the vertical slice method for the analysis of reinforced soil of unknown parameters being more than the number of equations available, is resolved by the horizontal slices method. The assumptions of HSM are (i) the vertical stress on an element in the soil mass is equal to the overburden pressure, (ii) the factor of safety (F.S.) is equal to the ratio of the available shear resistance to the mobilized shear stress along the failure surface, (iii) the factor of safety for all the slices is equal and (iv) the failure surface can have any arbitrary shape but does not pass below the toe of the slope or wall. Forces acting on a horizontal slice are shown in **Figure 12**.

With failure wedge divided into  $N$  horizontal slices,  $4N$  unknowns can be determined by  $4N$  equations and a complete formulation is possible. The formulation is simplified if only vertical equilibrium is considered for individual slices together with overall horizontal equilibrium for the whole wedge, no account being taken of moment equilibrium. In this case the number of equations and the number of unknowns get reduced to  $2N + 1$ . HSM was extended to design of RE walls considering oblique pull by Reddy et al. [54].

## 7. Reinforced slope with cohesive backfill

Reinforced Slopes are conventionally constructed with granular fill. However, this has limited the use of reinforced soil structures in locations where such free

draining backfill material is not readily available in close vicinity of the sites. Zornberg and Mitchell [55] and Mitchell and Zornberg [56] evaluated the use and performance of reinforced soil structures constructed with poorly draining and/or cohesive backfills. Permeable reinforcements are particularly appropriate for poorly draining backfills as they facilitate dissipation of excess porewater pressures.

## 7.1 Design methods

Christopher et al. [29] provide design guidance for reinforced soil structures using poorly draining backfills, viz., total stress analysis ignoring the drainage contribution of geocomposite for short term and effective stress analysis considering drainage in the long term. Naughton et al. [30] improved the design method of Christopher et al. [29] and presented single stage effective stress analysis since excess pore pressure gets dissipated fully before construction of subsequent layers. Half meter thickness of each lift is proposed to control short term stability of the slope face. Giroud et al. [32] updated design method of Naughton et al. [30] for reinforced slopes using draining geogrid with focus on an improved determination of the required transmissivity of the same. The method is practical as it makes it possible to optimize the design by adjusting the parameters such as the construction time, time required for pore pressure dissipation, layer thickness and drainage length. Naughton et al. [57] present a parametric study of design parameters of low permeability fill and concluded that for typical compressibility and consolidation parameters vertical spacing of the reinforcement of 0.5 m was adequate.

## 7.2 Design method - Giroud et al.

Giroud et al. [31, 32] presented a method for reinforced slopes using draining geogrid. Transmissivity and length of draining path are important for geogrids from the design point. Typical values of the parameters are:  $\phi$  ' of 20° to 30°, drained cohesion,  $c'$  of 0–20 kPa, coefficient of consolidation,  $c_v$  of 0.1–100 m<sup>2</sup>/year, and coefficient of compressibility,  $m_v$  of 0.01–5 m<sup>2</sup>/MN. Long term hydraulic transmissivity,  $\theta_a$ , of draining geogrid is obtained by applying a set of reduction factors to the laboratory measured value. Reduction factors account for creep, particulate, chemical and biological clogging of drainage channels.

Geometry of reinforced fill is important from design point of view. A drain located at the back of reinforced zone (**Figure 13**) is generally used to prevent groundwater from flowing into the reinforced zone and to halve the drainage length

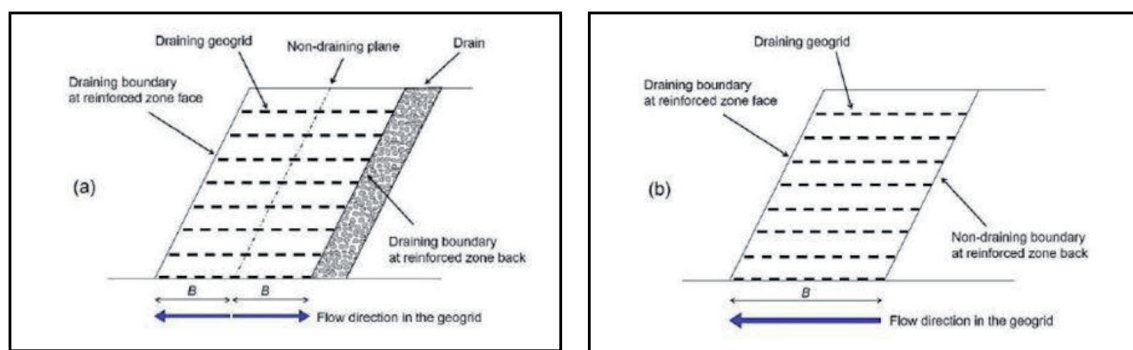


**Figure 13.**

*Geometry of reinforced slope with (a) and without drain (b) (after Naughton et al. [32]).*

in the draining geogrid. Design has two main components, viz., (i) determination of required transmissivity of draining geogrid and required time for rapid dissipation of porewater pressure and (ii) determination of stability and settlement of slope as in conventional practice.

The maximum porewater pressure in the drainage channel should not be too high nor too low. If the porewater pressure in the drainage channel is too high, vertical flow of water from the fill to the drainage channel will be slowed down, whereas, if the water pressure in the drainage channel is too low, flow of water will be too slow. Solution to this complex problem is presented by Giroud [58]. The rate of maximum vertical flow rate from fill to drainage channel depends on time factor ( $T_0 = 4C_v t_0 / H^2$ ) and occurs at the end of construction,  $t_0$ , of fill layer of thickness,  $H$ , overlying draining geogrid.

The following equations for the required transmissivity,  $\theta_{req}$ , are derived by Giroud [58], assuming that the maximum water pressure in the drainage channel,  $u_{max}$ , is 10% of the overburden stress, consistent with a degree of consolidation of 90% in the fill.

$$\theta_{req} = 10B^2k / H\sqrt{T_0} = 5B^2k / \sqrt{C_v t_0} \text{ if } 1 \times 10^{-6} \leq T_0 \leq 1 \quad (8)$$

and

$$\theta_{req} = 10B^2k / HT_0 = 5B^2k / 2C_v t_0 \text{ if } 1 \times 10^{-6} \leq T_0 \leq 1 \quad (9)$$

The required transmissivity,  $\theta_{req}$ , must be less than the allowable transmissivity,  $\theta_a$ . Parameter  $B$  in the above equation is dependent on length of draining geogrid. In case of draining boundary at the back of the reinforced zone (**Figure 13**) drainage path length is equal to half and in case of non-draining boundary it is equal to full length of reinforcement. The required transmissivity depends on hydraulic gradient in the drainage channel. An approximate value of hydraulic gradient in the drainage channel is given by

$$i_{avg} = u_{max} / \gamma_w B \quad (10)$$

where  $u_{max}$  is maximum allowable water pressure in drainage channel and is generally taken as 10% of overburden stress. The time required for pore water pressure dissipation is estimated as time required to reach 90% consolidation and is calculated as under

$$t_{90} = \frac{T_{90} H^2}{4C_v} \quad (11)$$

where  $T_{90}$  is time factor for 90% consolidation. The parameter  $B$  is equal to the length of reinforcement and is obtained as part of stability analysis (Jewell [14]). Alternatively, the geogrid length is selected arbitrarily and stability is checked separately.

### 7.2.1 Parametric study

Naughton et al. [32] conducted parametric studies to study time for pore pressure dissipation, and required transmissivity of the geogrid. From practical consideration, construction of one layer per day implies about 24 hours for porewater

pressure dissipation. Studies reveal that this is achievable unless  $c_v$  is less than  $30 \text{ m}^2/\text{year}$  and vertical spacing is more than  $0.5 \text{ m}$ . For  $c_v$  values greater than  $50 \text{ m}^2/\text{year}$  and thickness of fill not exceeding  $0.5 \text{ m}$ , the dissipation time required reduces to less than 12 hours (**Figure 14**).

For soils with  $c_v$  up to  $50 \text{ m}^2/\text{year}$ , the unfactored required transmissivity in the draining geogrid is less than  $1.2 \times 10^{-6} \text{ m}^2/\text{s}$ . As the drainage characteristic of the soil improves, i.e.,  $c_v > 75 \text{ m}^2/\text{year}$ , the required transmissivity increases rapidly by orders of magnitude (**Figure 15**). The required transmissivity also depends on the vertical spacing of the draining geogrid.

Smaller vertical spacings and longer reinforcement lengths require larger transmissivity in the draining geogrid. Reinforcement spacing of  $0.5 \text{ m}$  optimizes the time for dissipation of pore pressures while, at the same time, requiring realistic and achievable transmissivity in the draining geogrid.

At this spacing a draining geogrid will dissipate pore pressures over the full range of likely values encountered in low permeability fills within 24 hours, with the further advantage that the required transmissivity is independent of reinforcement length. With above spacing, reinforced slope with poorly draining backfill can be analyzed as a normal slope for both internal and external stability for normal ranges of soil parameters.

### 7.3 Semi-analytical design method for cohesive backfill reinforced slope

Abd and Utili [33] developed a semi-analytical method for uniform slope with  $c-\phi$  soil using Limit Analysis (LA). The method provides the amount of reinforcement needed as a function of cohesion, tensile strength, angle of shearing resistance and slope inclination. Climate induced crack and cracks that form due to slope collapse are accounted for in this method. Both soil and reinforcement are assumed to be rigid-plastic and follow normality rule i.e., associated plastic flow.

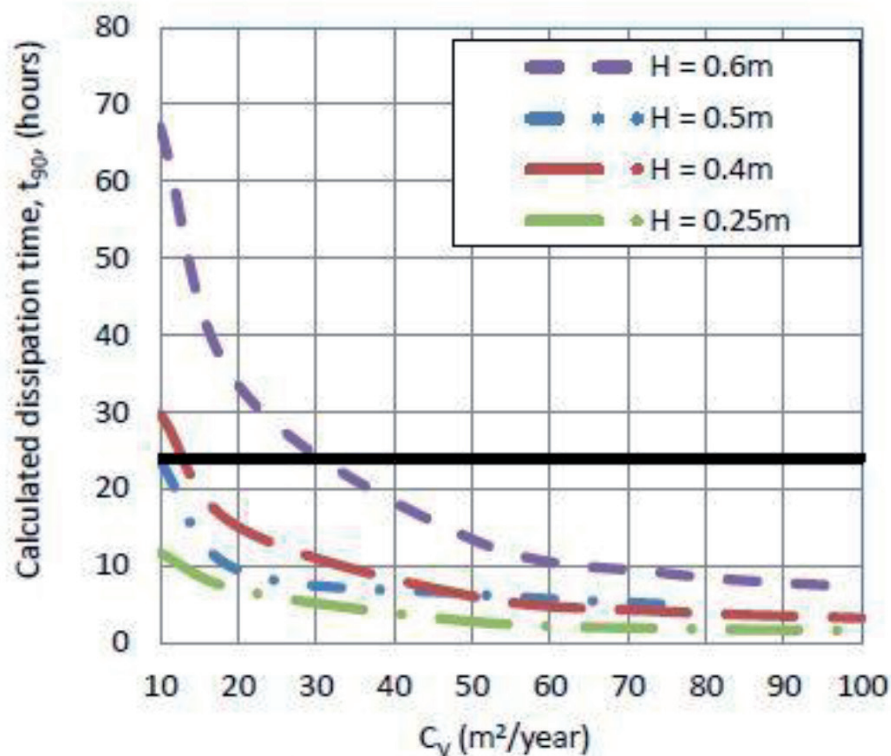


**Figure 14.** Variation of dissipation time ( $t_{90}$ ) with coefficient of consolidation ( $c_v$ ) for reinforcement length equal to height of slope (after Naughton et al. [32]).

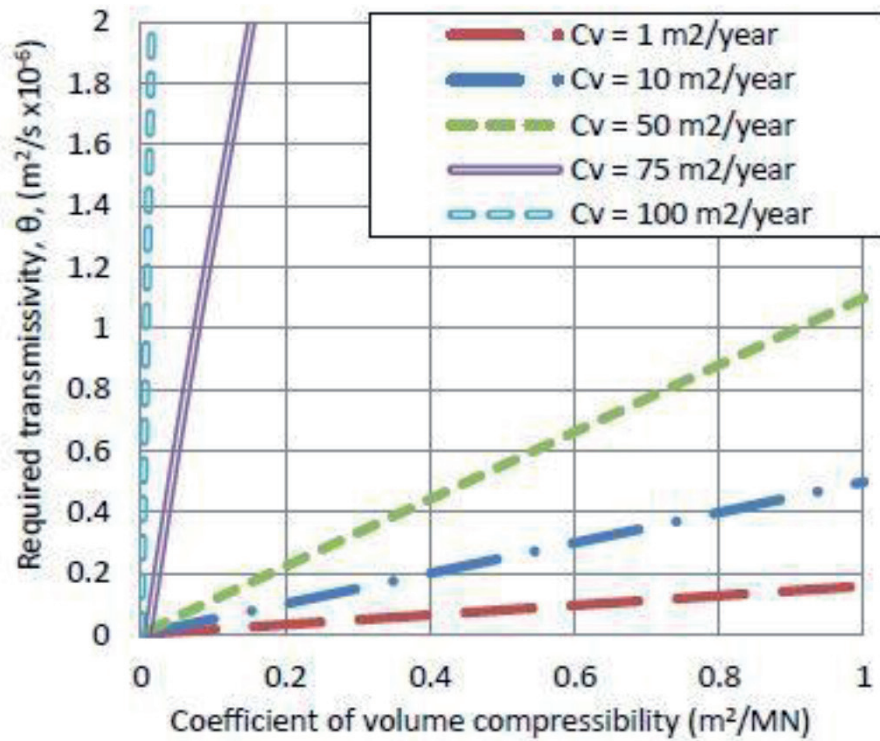


**Figure 15.** Variation of required transmissivity of the geogrids,  $\theta$ , with coefficient of volume compressibility,  $m_v$ , for a range of coefficients of consolidation, reinforcement length =  $1.0H$  (after Naughton et al. [32]).

### 7.3.1 Design

Traction free slopes with slope angle of  $40-90^\circ$  reinforced with geosynthetic layers are considered. Reinforcement is equally spaced throughout (uniform distribution - UD) or at a spacing decreasing from top to bottom of slope (Linearly Increasing Distribution - LID) (**Figure 16**).

Average strength of reinforcement,  $K_t$ , for UD case is

$$K_t = nT / H \quad (12)$$

where  $n$  - the number of reinforcement layers,  $T$  - the strength of a single layer at yield and  $H$  - the slope height.

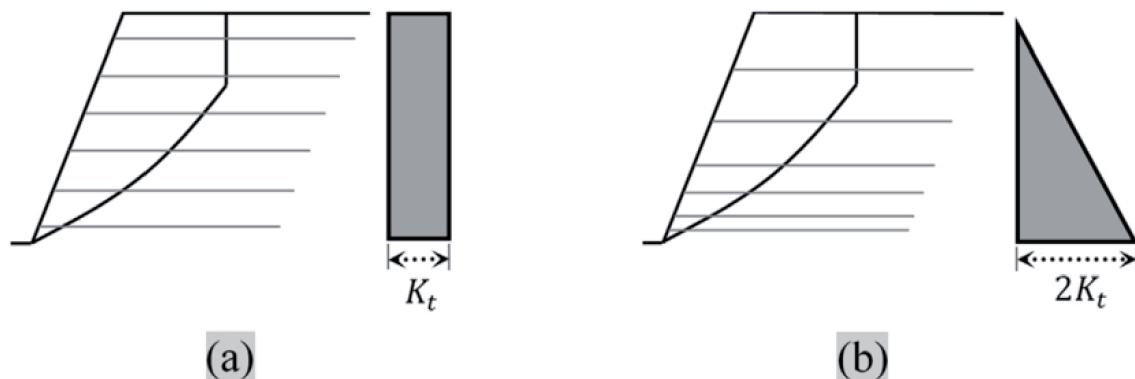


**Figure 16.** Geosynthetic-reinforcement layouts: (a) uniform and (b) linearly increasing distribution with depth (after Abd. and Utili [57]).

For LID case local reinforcement strength,  $K$ , is

$$K = 2K_t (H - y) / H \quad (13)$$

where  $y$  - the vertical coordinate from the slope toe. Maximum depth of crack is limited from the requirement that remaining slope remains stable. Upper bound maximum crack depth to be adopted [59] is

$$h_{\max} = \frac{3.83c \tan\left(\frac{\delta}{4} + \frac{\phi}{2}\right)}{y} \quad (14)$$

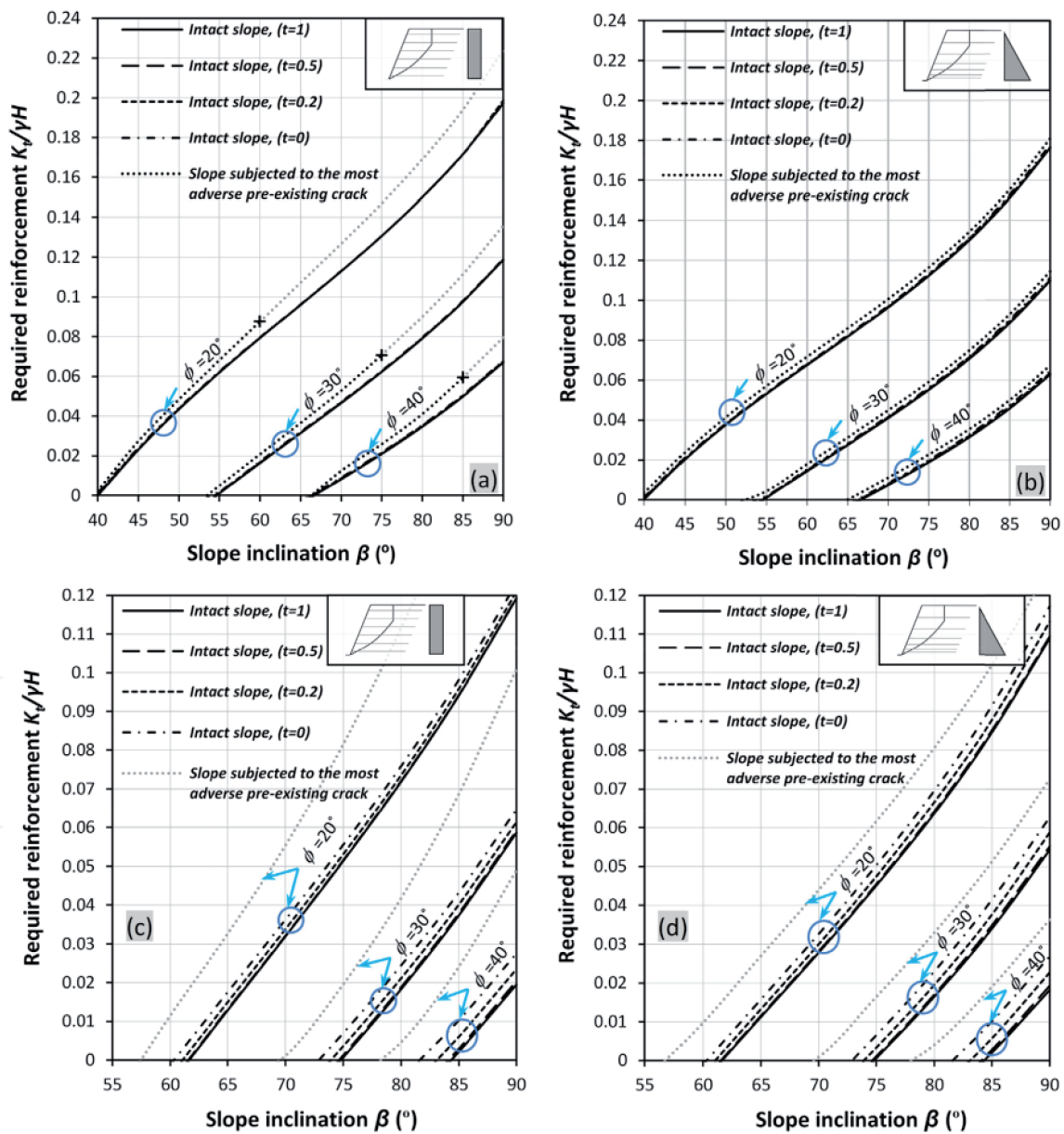


**Figure 17.** Design charts for intact slopes not subject to crack formation ( $t = 1$ ), intact slopes subject to crack formation (limited tensile strength of  $t = 0.5$ ,  $t = 0.2$  &  $t = 0$ ) and cracked slopes. (a) & (b) are for  $c/\gamma H = 0.05$  while (c) & (d) are for  $c/\gamma H = 0.1$ . (after Abd and Utili [33]).

### 7.3.2 Required reinforcement

Design charts (**Figure 17**) provide the reinforcement strength and embedment length for uniform and linearly increasing reinforcement distributions for different slope angles  $\beta$  and  $\phi$  for specified value of  $c/\gamma H$ .

In **Figure 17**, 't' is dimensionless coefficient representing soil tensile strength and is defined as ratio of ground tensile strength to be measured experimentally over maximum unconfined tensile strength consistent with Mohr-Coulomb criteria. Considering the case of intact slopes, it can be observed that for relatively low values of cohesion,  $c/\gamma H = 0.05$ , the tensile strength, t, has negligible effect on the required reinforcement force. But for higher values of cohesion ( $c/\gamma H = 0.1$ ), t becomes important. Above charts are for fully drained slopes.

Using **Figure 17**,  $K_t/\gamma H$  can be determined for given slope angle,  $\beta$ , and angle of shearing resistance,  $\phi$ , of soil. Tensile strength of reinforcement is calculated using Eq. 10 for given number of layers. Influence of porewater pressure on required amount of reinforcement is analyzed using  $r_u$  method [60]. A uniform value of  $r_u$  is assumed throughout the slope and effective stress analysis carried out. **Figure 18** provides  $K_t/\gamma H$  for slope inclinations of  $40^\circ$  to  $90^\circ$ ,  $r_u = 0, 0.25$  and  $0.5$  for UD and LID cases.

Gray and black lines in **Figure 17** indicate respectively active and inactive constraint of maximum crack depth. The mark + signals the boundary between the two.

Gray and black lines in **Figure 18** indicate respectively active and inactive constraint of maximum crack depth. The mark + signals the boundary between the two (after Abd and Utili [33]).

A combined failure mode consisting of pullout in some layers and rupture (tensile failure) in others, also needs to be considered to calculate the minimum length of the reinforcement layers. **Figure 19** provides  $L_r/H$  as a function of slope angle,  $\beta$  for  $\phi$  of  $20^\circ$  for this case.

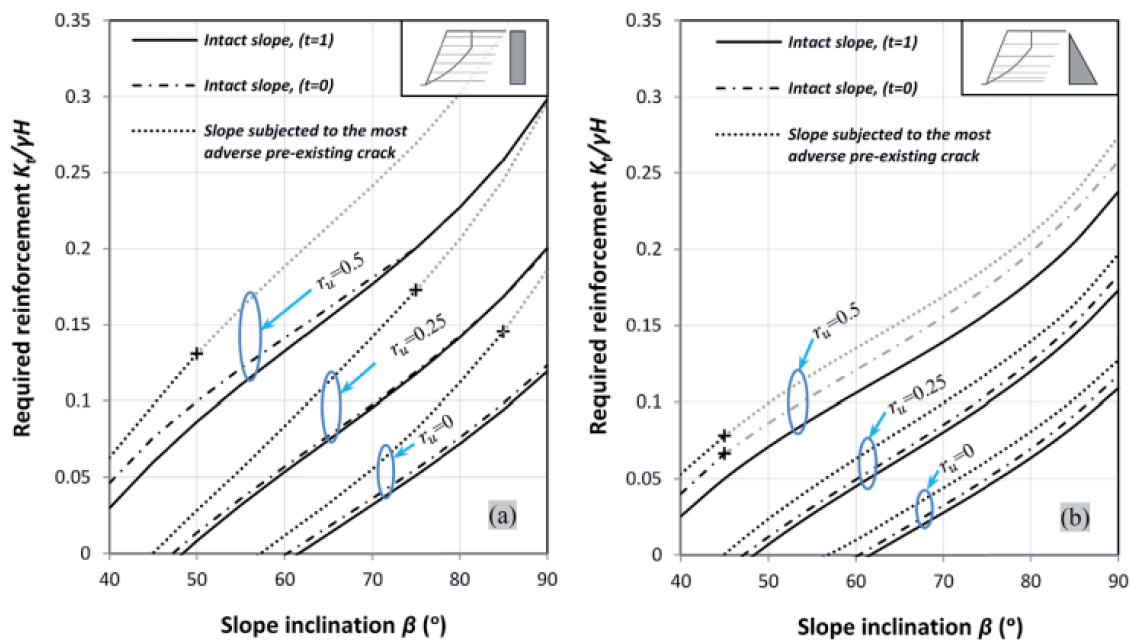


**Figure 18.**  
 Design charts for the required reinforcement for intact and cracked slopes (with  $\phi = 20^\circ$  and  $c/\gamma H = 0.1$ )  
 (a) UD of reinforcement; and (b) LID.

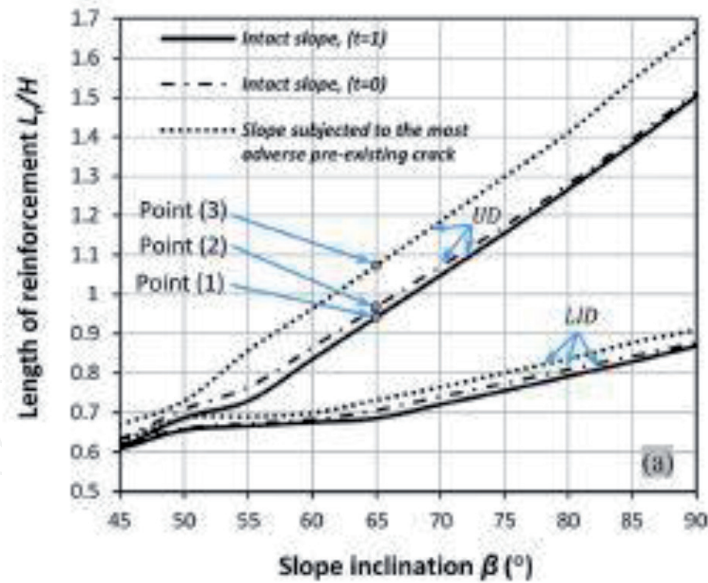


**Figure 19.**

Length of reinforcement for a slope with  $\phi = 20^\circ$ ,  $c/\gamma H = 0.05$  and  $r_u = 0$ .

## 8. Slope - reinforcement interaction and length optimization

The inclusion of geosynthetic reinforcement in soil slope for improving stability leads to change in behavior of reinforced soil mass due to induced stresses as compared to that in unreinforced slope so far as critical slip circle is concerned. Hence there is a need to understand slope-reinforcement interaction behavior. Jha et al. [61–64] optimized reinforcement length from face of slope and identified and quantified slope-reinforcement interaction.

To study soil reinforcement interaction and length optimization reinforced embankment slope, on a competent soil, 6.0 m high with side slope of 1.5H:1 V is considered (**Figure 20**).

The embankment and foundation soil have cohesion,  $c$ , of 5 kPa, unit weight,  $\gamma$ , of  $18 \text{ kN/m}^3$  and angle of shearing resistance,  $\phi$ , of  $23^\circ$ . The geotextile reinforcement used has adhesion,  $c_a$ , of 3 kPa, angle of interface friction between soil and reinforcement,  $\delta$ , of  $17^\circ$  and ultimate tensile strength,  $T_{ult}$ , of 200 kN/m.

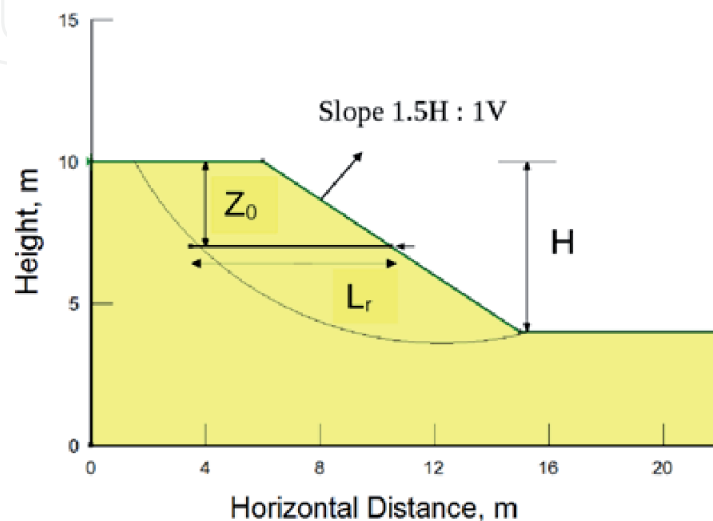


**Figure 20.**

Schematic diagram - reinforced embankment slope.

Analysis of unreinforced embankment of 6 m leads to  $FS_{min}$  of 1.22 less than the required value of 1.3 and hence needs to be reinforced with geosynthetic reinforcement to get preferably long term  $FS_{min}$  of 1.5.

### 8.1 Reinforcement length optimization: non-face end

Effect of varying the length,  $L_r$ , of geosynthetic placed at depth,  $Z_0 = 3.0$  m in 6.0 m high embankment is studied by curtailing it from the non-slope face to get  $FS_{min}$  in the range of 1.50 to 1.60. The length,  $L_r$ , of the reinforcement to intercept the failure surface at 3.0 m depth was varied from 8.0 m with  $FS_{min}$  of 1.6 (Figure 21).

Circles ABC and DEF are the critical slip circles of the unreinforced and the reinforced slopes. One of the effects of inclusion of reinforcement in embankment soil is to shift the critical slip circle from ABC to DEF, that is from shallower to deep inside the slope. This shift of the critical circle therefore increases the factor of safety by involving larger slide mass. PQ is reinforcement of length  $L_r$ . The length of reinforcement  $L_r$  has two components:  $QE =$  effective length,  $L_e$ , in the stable zone and  $EP =$  the length,  $L_f$  in the unstable zone.  $L_f$  is further divided into lengths  $L_{f1}$  (EB), the length in the failure zone between the critical slip circles of the reinforced and the unreinforced slopes and length,  $L_{f2}$ , between the critical slip circle of unreinforced slope and slope face (BP) as shown in Figure 21. The effect of varying  $L_r$  with right end fixed at point P and left end (Q) curtailed inwards successively, leads to reduction in mobilized force in the reinforcement ( $F_r$ ) from 35.8 kN/m to 19.6 kN/m corresponding to reduction in  $L_r$  from 8.0 to 7.3 m.  $FS_{min}$  reduces from 1.60 to 1.51. Factor of safety and the load/resistance mobilized in the reinforcement decrease with reducing length of reinforcement as is to be expected.  $FS_{min}$  falls below 1.50 on reducing the length further to 7.0 m.

### 8.2 Length optimization from face end

The length,  $L_f = (L_r - L_e)$  is much larger than  $L_e$ , the effective length of reinforcement contributing to increase in the stabilizing moment/force. The required pullout force in the reinforcement in the stable zone should equal to that mobilized by the corresponding length of the reinforcement in the unstable zone for equilibrium. It would serve no useful purpose if the length of the reinforcement in the unstable

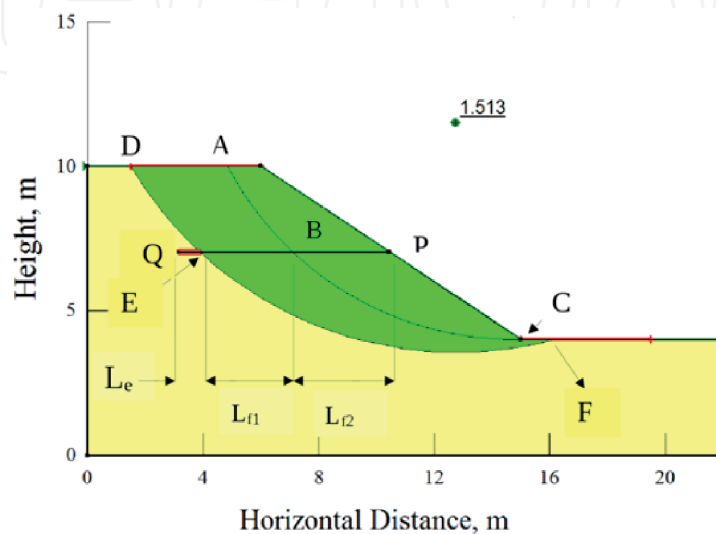


Figure 21.  
 Critical slip circle for  $Z_0 = 3.0$  m,  $FS_{min} = 1.51$ ,  $L_r = 7.27$  m.

zone is more than that required for generating the required stabilizing force. Hence minimizing  $L_f = (L_r - L_e)$  by moving point P inside the soil mass and away from the slope face by curtailing length of reinforcement but still maintaining  $FS_{min}$  above 1.50 can lead to economy. Accordingly, for reinforced slope of **Figure 21**,  $L_r$  has been curtailed from the face end of the slope. As point P is moved inside gradually by reducing  $L_r$ , the critical circle continues to be DEF or close to it (**Figure 22**), i.e., practically with no shift of the critical circle.

The minimum length,  $L_r$  which provides  $FS_{min} = 1.51$  is obtained as 5.08 m (**Figure 22**). Thus about 30% reduction in length of reinforcement is achieved without sacrificing the stability of the embankment slope as  $FS_{min}$  is still the required value of 1.5. Hence length optimization from face end leads to saving of reinforcement length. The circle, ABC, is not the critical for the reinforced slope and thus not acceptable as the critical circle with consideration of reinforcement is different from that of unreinforced case.

### 8.3 Slope-reinforcement interaction

Slope as in **Figure 21** has been analyzed further for the critical slip circle DEF of reinforced slope but without considering the effect of reinforcement to get FS of 1.41 (**Figure 23**).

The summary of results for various depth of reinforcement from top of embankment is summarized in **Table 5**.

The contribution of reinforcement in enhancing the stability of a slope is observed to be twofold: (i) shifting of the critical slip circle deeper in to the slope involving larger slide mass or forward involving smaller slide mass and thus enhancing the factor of safety of the slope and (ii) due to contribution of reinforcement to stabilizing force/moment.  $FS_{min}$  of 1.22 for unreinforced case increases to 1.41 due to shifting of the critical circle to DEF an increase of 15.6%. Secondly the contribution of reinforcement to stabilizing moment/force leads to a further increase in factor of safety from 1.41 to 1.51, a contribution of about 8.2%.

### 8.4 Summary of slope -reinforcement interactions

Slope - reinforcement interaction analysis is summarized as follows: (i) The critical slip circle for the slope with reinforcement shifts inward and is very different

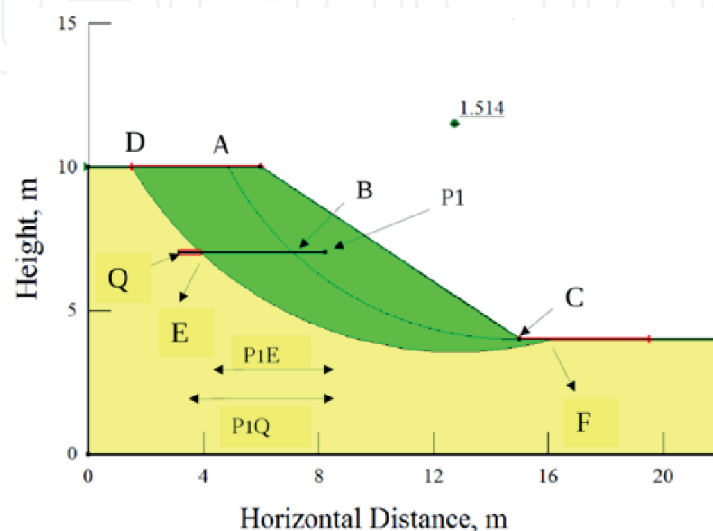


**Figure 22.**  
Critical slip circle for slope with  $Z_o = 3.0$  m,  $L_r = 5.08$  m and  $FS_{min} = 1.51$ .

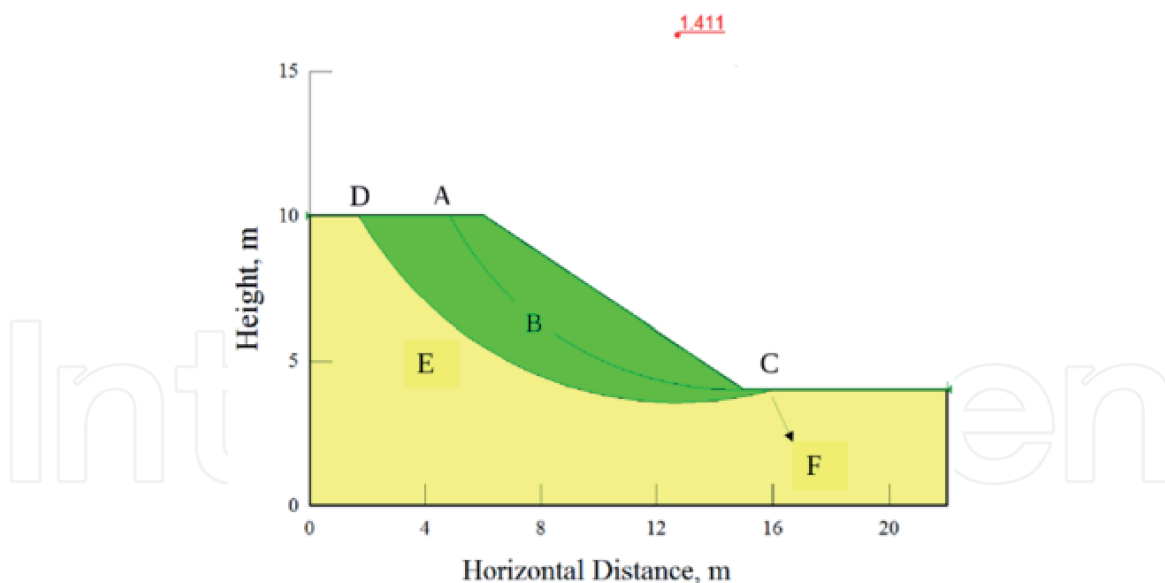


**Figure 23.**  
 Slope stability with critical slip circle DEF but without considering the effect of reinforcement.

$Z_0, \text{m}$	FS				$L_r, \text{m}$
	I	II	III	IV	
3.0	1.22	1.51	1.80	1.41	5.08
4.0	1.22	1.51	1.86	1.48	5.26
5.0	1.22	1.51	1.92	1.46	6.04

I:  $FS_{min}$  for unreinforced slope with critical circle ABC; II:  $FS_{min}$  for reinforced slope with critical circle DEF; III: FS for reinforced slope analyzed for circle ABC of unreinforced slope and IV: Reinforced slope analyzed for critical slip circle DEF but without considering the effect of reinforcement.

**Table 5.**  
 Factors of safety and lengths of Geosynthetics.

from that for the unreinforced slope; (ii) The increase in factor of safety is because of the shift of the critical slip circle deep in the slope and involving larger sliding mass. This results from the fact that the slip circle is deeper in to the soil and away from the critical circle corresponding to that for unreinforced embankment soil; As a consequence, the reinforcement force generated becomes much smaller than that estimated based on the length corresponding to that estimated with respect to slip circle for the unreinforced slope; (iii) The effect of providing reinforcement in the slope is two-fold, viz., shifting of critical circle inside of the embankment involving larger slide mass and by increase in stabilizing force/moment due to bond resistance mobilized in the reinforcement; and (iv) It is possible to achieve about 20 to 30% shorter length of the reinforcement without endangering the stability of the embankment slope. The most significant finding of this study is that the reinforcement can be provided from inside and not necessarily from the face of the embankment.

## 9. Software for analysis of reinforced slope

The objective in designing geosynthetic reinforced soil slope is to determine the required long-term strength and layout of the reinforcement apart from finding the critical failure surface. The layout and strength are interrelated rendering many

possible solutions with the same level of stability but not necessarily having the same economics. Software facilitates the designer to reach an optimal solution apart from locating critical failure surface by using search techniques and by repeatedly performing the stability calculations for different failure surfaces.

Pockoski and Duncan [65] compared several Limit Equilibrium based software available based on features of program, ease of use, range of applicability, accuracy, and efficiency. These programs were rated as well considering accuracy of results, computation time, learning curve, time to enter data and complete an analysis, ease of reinforced slope design, ease of unreinforced data entry, time required to make graphical output Report -Ready and quality of output. Different software included for comparison are: UTEXAS4 & TEXGRAF4, SLOPE/W, SLIDE, XSTABL, WINSTABL, RSS, SNAIL, GoldNail. UTEXAS4 is a precise analysis tool but does not have graphic user interface. TEXGRAF4 is second part of UTEXAS software package and displays information and results of the UTEXAS4 search and generates file for use in CAD software. SLOPE/W having a graphic user interface is user friendly and versatile. Reinforcement inclusion in to the analysis is also graphical. SLOPE/W has Monte Carlo based probabilistic stability analysis option where by soil, porewater pressure and seismic coefficient can be entered with standard deviation. SLIDE is Windows based slope stability program and can search for a critical circular, non- circular or composite slip surfaces. XSTABL is an interactive program which can search critical circular surface. WINSTABL is windows-based program whereby geosynthetic reinforcement, anisotropic soil, seismic loads, etc. can be considered in the analysis. RSS is an interactive program and is capable of exhaustive search performed on reinforced slope. Circular, bilinear, bottom third and top third failure surfaces are considered. SNAIL is window based free software and permits use of seven different types of soils and uses force equilibrium on two and three-part wedge analysis. GoldNail is a very powerful and design program that is primarily meant for soil nail wall analysis.

SSAP release 5.0 (2020) software (<https://www.ssap.eu>) is a versatile free software and uses advanced limit equilibrium method and FE-LEM combination to get the critical Factor of safety. ReSlope is an interactive, design-oriented, program for geosynthetic-reinforced slopes. For a given problem including geosynthetic strength, reduction factors, and design safety factors, ReSlope produces the optimal layout (i.e., length and spacing) of reinforcement layers. ReSlope was specifically developed for geosynthetics. SVSLOPE, GeoStru, Oasys, ReActive, Secuslope are other software available for reinforced slope stability analysis.

## 10. Case studies and lessons learnt

Liu et al. [66] studied failure of a four-tiered geogrid reinforced slope of a road embankment of height varying from 10 m to 40 m over a length of 430 m to assess mechanism and causes contributing to these failures (**Figures 24 and 25**). A flat natural slope of  $28^\circ$  was converted to a steep geogrid reinforced slope of 0.5 H:1 V ( $63^\circ$ ) slope for constructing an approach road.

The first slope failure occurred during the construction phase itself soon after the rainy season as rainwater seeped into permeable laterite gravel layer underlain by an impermeable clay layer. The interface of laterite gravel and clay created a detrimental bedding plane whose shear strength was reduced due to infiltration of water. The slide got initiated along the interface when toe was excavated to construct the reinforced zone. The second failure occurred due to very strong earthquake. The overstress initiated near the vicinity of the clay layer extended into the retained natural slope to form a massive slide. The third failure occurred following

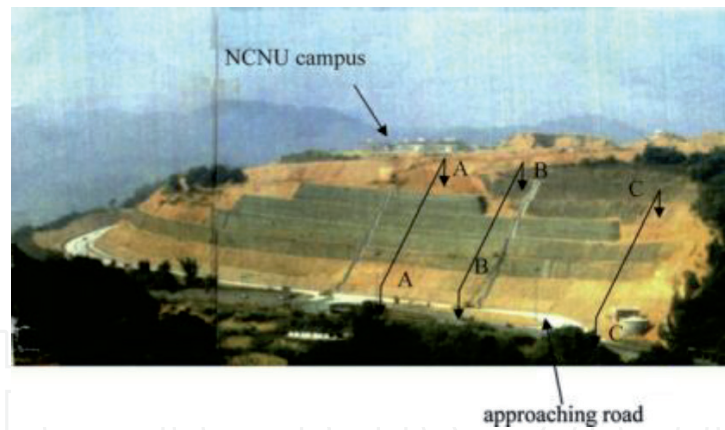


Figure 24.  
Approach road (after [66]).

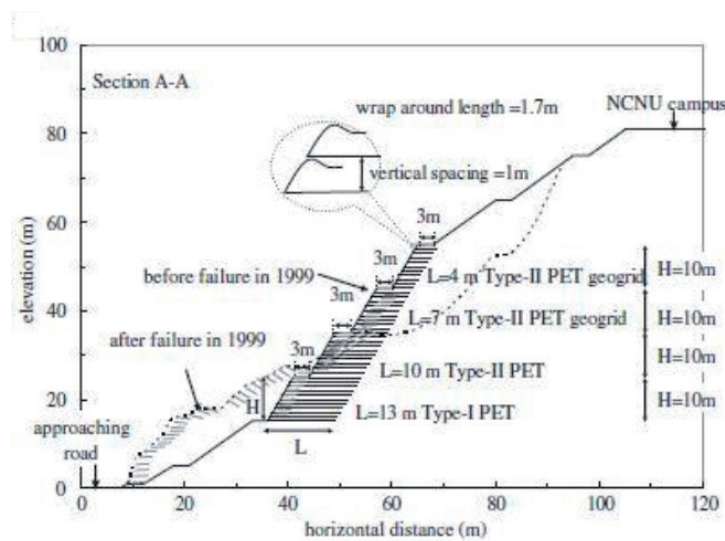
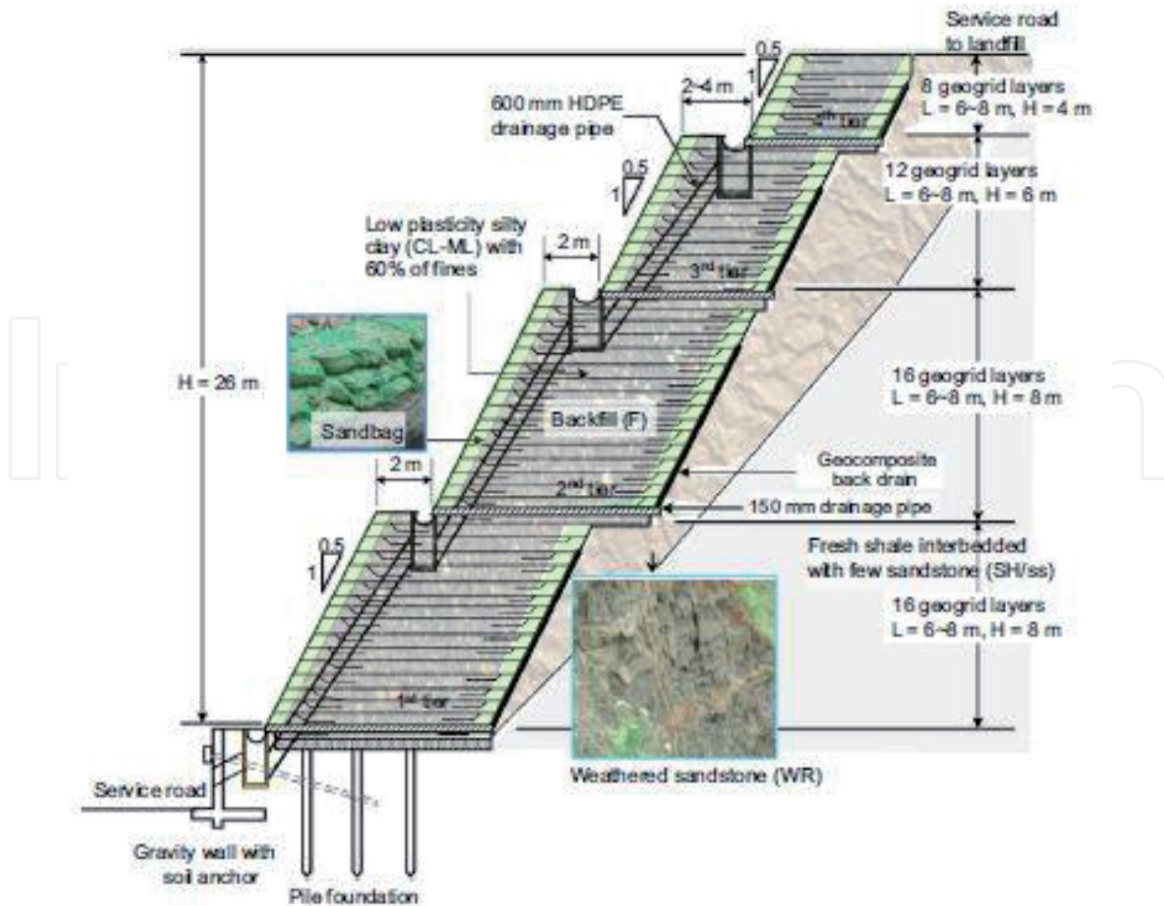


Figure 25.  
Reinforced slope with failure details (after [66]).

abundant rainfall during a heavy rainstorm that infiltrated into the reinforced slope as no sub-drainage system was provided. The infiltration that was obstructed by the impermeable clay and fine contents in the backfills generated significant water pressure, inducing the slope to fail behind the reinforced zone.

The interface between laterite gravel and clay is an embedded weak plane, which when saturated softened. In addition, because of its low permeability, it became a barrier to the infiltration. Site investigation failed to find the existence of this clay layer, because the reinforced slope was thought to be subsidiary to campus buildings, and no investigation efforts made specific to the reinforced structures. The succeeding design and construction did not appropriately correspond to this clay layer even when it was observed during construction. The results showed the impact of the clay layer on the slope stability to be very critical. The current practice of considering cohesion needs to be re-evaluated as this apparent cohesion may get reduced to even zero with increasing saturation. The lack of a drainage system was another significant cause for failure.

Yang et al. [67] investigated 26 m high, four-tier geogrid reinforced slope (Figure 26), backfilled with low plasticity silty clay that contains more than 60% of fines (marginal backfill). Prior to the completion of construction, tension cracks were discovered along with slope settlement at the top of the slope. The tension cracks and slope settlement were caused by a series of heavy rainfall. The slope



**Figure 26.**  
*Layout and Design of Multitier Geosynthetic Reinforced Slope (after [67]).*

settlement was repaired by placing additional backfill on the top of the slope to compensate for the settlement that had occurred.

During the next rainy season, the slope was subjected to a significant amount of rainfall of 187 mm in May, 350 mm in June, 243 mm in July, and 563 mm in August. During this period, tension cracks and slope settlement got regenerated and gradually developed as the rainfall continued. **Figure 27** displays subsequent development of the tension cracks and slope settlement with time.

Factors that caused the slope failure from the forensic investigation are: (i) The use of marginal soil (over 60% of fines) as the backfill without provision of drainage. (ii) The original design and site investigation overlooked the existence of the weathered and fractured rock layer, which has shear strength less than that of an intact rock. (iii) Tension cracks and slope settlement developed at the top surface of the slope allowed rainwater to pond on the top and to infiltrate into the reinforced zone. (iv) The drainage system may have malfunctioned as joints were poorly and loosely connected and likely got dislocated due to the excessive deformation.

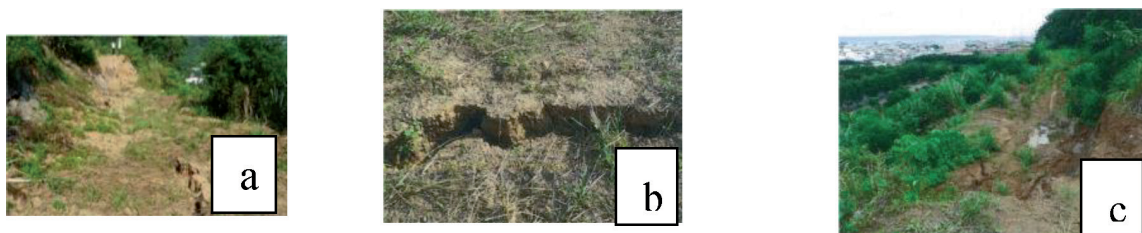


**Figure 27.**  
*Tension crack and settlement of slope and its failure after rains of 2012 (a) tension crack; (b) onset of settlement; (c) excessive settlement over 1 m (after [67]).*

Lessons learnt from these case histories are: (i) Detailed site investigation should be carried out to assess presence of weak layer, soil weathered rock, etc., (ii) Design cohesive backfill slope for drainage and with provision of draining geosynthetics, (iii) Install drainage systems appropriately and (iv) Design RE slope for global stability.

However, it is pertinent to mention that marginal soil can be used with draining geogrids as detailed in Section 7.2 with adequate drainage capacity.

## 11. Conclusions

Steep slope embankment is a necessity for development of rail, road and other infrastructure projects. Safety of embankment slopes is of utmost importance which requires proper site investigation, analysis and design. Limit Equilibrium, Limit Analysis, Slip Line & Finite Element Methods are design methods for RE Slopes. Limit equilibrium method is most commonly used for design including the effect of reinforcement. Jewell's design method [14] for geosynthetic reinforced steep slope soil with granular soil is most commonly used method. Song et al. [28] proposed new approach based on LE principle to evaluate stability of reinforced slope. Slopes with cohesive backfill have been constructed due to limited availability of granular material near project site. Proper design of RE slope using cohesive backfill considering the transmissivity of draining geogrid is important. The method suggested by Giroud et al. [32] for draining geogrid reinforced cohesive back fill slope with 0.5 m/day is practical method as it takes care of pore water pressure dissipation for most common soil parameters. Abd & Utili [33] developed a semi-analytical method for uniform slope with  $c-\phi$  soil using Limit Analysis (LA). The method provides the amount of reinforcement needed as a function of cohesion, tensile strength, angle of shearing resistance and slope inclination. The reinforcement length optimization from face end leads to economy in reinforcement length of the order of 20–30% without affecting factor of safety [61]. There is an interaction between slope and reinforcement [62, 64]. Inclusion of reinforcement in embankment slope results in shifting of critical slip circle deep inside slope involving larger slide mass thus increasing factor of safety. Reinforcement also provides stabilizing moment/force. Investigation of failed slopes indicate that detailed geotechnical investigation of site to assess presence of weak layer, provision of drainage by way of draining geosynthetics in case of cohesive backfill, installation of drainage systems to capture rain and subsurface water and global stability of reinforced earth slopes are very critical for stability and performance of reinforced slope.

## Acknowledgements

I express my sincere thanks to Prof M.R. Madhav my mentor and Co-author of this chapter whose continued encouragement and support made it possible to complete the chapter and bring it to the current format. I am also thankful to my wife Abha who always supported me in this endeavor. I thank Ms. B. Geeta Sahithi my office colleague for helping me for improved figures out of her personal time.

IntechOpen

### Author details

Akshay Kumar Jha<sup>1\*</sup> and Madhav Madhira<sup>2</sup>

1 Indian Railways, Hyderabad, India

2 Department of Civil Engineering, I.I.T. Hyderabad and JNTU, Hyderabad, India

\*Address all correspondence to: akshayghunru@gmail.com

### IntechOpen

---

© 2020 The Author(s). Licensee IntechOpen. This chapter is distributed under the terms of the Creative Commons Attribution License (<http://creativecommons.org/licenses/by/3.0>), which permits unrestricted use, distribution, and reproduction in any medium, provided the original work is properly cited. 

## References

- [1] Petley DN, Dunning SA, Rosser NJ (2005). The analysis of global landslide risk through the creation of a database of worldwide landslide fatalities. In: Hungr O, Fell R, Couture R, Eberhardt E (eds) *Landslide risk management*. CRC Press, London, p. 367-373.
- [2] Nadim F, Kjekstad O (2009). Assessment of Global High-Risk Landslide Disaster Hotspots. In: Sassa K, Canuti P (eds) *Landslide- Disaster Risk Reduction*. Springer, Berlin, p. 213-221.
- [3] Simac, M.R. (1992). Reinforced slopes: a proven geotechnical innovation. *Geotechnical Fabrics Report*, p. 13-25.
- [4] Zeynep, D. and Tezcan, S. (1992). Cost analysis of Reinforced soil walls. *Geotextiles and Geomembranes* 11. p. 29-43.
- [5] Lostumbo, J. M. (2010). The Yeager Airport Runway Extension: Tallest 1H: 1V Slope in US Case Study *Advances in Analysis, Modeling and Design*. GSP No.199 ASCE, GeoFlorida, p. 2502-2510.
- [6] Devata, M. S (1985). Geogrid reinforced earth embankments with steep side slopes. *Polymer Grid Reinforcement*, Thomas Telford Limited, London, p. 82-87.
- [7] Gharpure A., Kumar S.& Scotto M. (2012). Composite soil reinforcement system for retention of very high and steep fills –A case study. *Proceedings Vol 5. Topic: soil improvement and reinforcement. 5th European Geosynthetics Congress. Valencia 2012*. P. 346-352.
- [8] Jewell, R.A., Paine, N., and Wood, R.I. (1984). Design Methods for Steep Reinforced Embankments. *Proc. of the Polymer Grid Reinforcement Conf.*, London, p. 70-81.
- [9] Bonaparte, R., Holtz, R.D. and Giroud, J.P. (1987). Soil reinforcement design using geotextile and geogrids. *Geotextile Testing and Design Engineer*, ASTM STP 952, J. E. Fluet, Jr., Ed., American Society for Testing Materials, Philadelphia, p. 69-116.
- [10] Verduin, J.R. and Holtz, R.D. (1989). Geosynthetically reinforced slopes: A new Procedure. *Proc. Geosynthetics'89*. San Diego, IFAI, p. 279-290
- [11] Leshchinsky D, Reinschmidt AJ (1985). Stability of membrane reinforced slopes. *J Geotech Eng. ASCE* 111(11). p. 1285-1300
- [12] Leshchinsky, D. and Boedeker, R.H. (1989). Geosynthetic reinforced soil structures. *J. of Geotechnical Engineering*. 115(10). P. 1459-1478.
- [13] Schneider, H.R and Holtz, R.D. (1986). Design of Slopes reinforced with geotextiles and geogrids. *Geotextiles and Geomembranes*. 3. P. 29-51
- [14] Jewell, R.A. (1991). Application of the Revised Design Charts for Steep Slopes. *Geotextiles and Geomembranes*. 10(1091). p. 203-233.
- [15] Leshchinsky, D. (1992). Issues in Geosynthetic Reinforced Soil. *Earth Reinforcement Practice. Proc. of the International Symposium on Earth Reinforcement Practice*. Kyushu University, Fukuoka, Japan, Vol. 2, p. 871-897.
- [16] Leshchinsky, D., Ling, H. and Hanks, G. (1995). Unified design approach to geosynthetic reinforced slope and segmental walls. *Geosynthetics Int.*2(5). p. 845-881
- [17] Zhao A (1996) Limit Analysis of geosynthetic reinforced slopes. *Geosynth. Int.* 3(6). p. 721-740

- [18] Michalowski, R. L. (1997). Stability of uniformly reinforced slopes. *J. of Geotechnical and Geoenvironmental Engineering*, 23(6). p. 546-556.
- [19] Shiwakoti, D.R., Pradhan, T.B.S. and Leshchinsky, D. (1998). Performance of geosynthetic - reinforced soil structures at limit equilibrium state. *Geosynthetics International*, 5(6), p. 555-587.
- [20] Baker, R. and Klein, Y. (2004a). An integrated limiting equilibrium approach for design of reinforced soil retaining structures: Part I – Formulation. *Geotextiles and Geomembranes*, 22(3), p. 119-150.
- [21] Baker, R. and Klein, Y. (2004b). An integrated limiting equilibrium approach for design of reinforced soil retaining structures: Part II – Design examples. *Geotextiles and Geomembranes*, 22(3), p. 151-177.
- [22] Han, J. and Leshchinsky, D. (2006), "General analytical framework for design of flexible reinforced earth structures", *J. of Geotechnical and Geoenvironmental Engrg. ASCE*, 132, 1427-1435.
- [23] Leshchinsky, D., Zhu, F. and Meehan, C.L. (2010). Required unfactored strength of geosynthetic in reinforced earth structures. *J. of Geotechnical and Geoenvironmental Engineering*, 136(2), p. 281-289.
- [24] Leshchinsky, D., Kang, B., Han, J. & Ling, H. (2012). Framework of Limit State Design of Geosynthetic Reinforced Walls & Slopes. *Transp. Infrastructure Geotech.*, 1, p. 129-164.
- [25] Leshchinsky, B. and Ambauen, S. (2015) Limit equilibrium and limit analysis: comparison of benchmark slope stability problems. *ASCE J. of Geotechnical and Geoenvironmental Engineering*, DOI: 10.1061/(ASCE)GT.1943-5606.0001347.
- [26] Shukla, S.K., Sivakugan, N. and Das, B.M. (2011). A State-of-art review of geosynthetic-reinforced slope. *Int. J. of Geotechnical Engineering*, 5, p. 17-32
- [27] Gao, Y., Yang, S., Zhang, F. and Leshchinsky, B (2016). Three dimensional reinforced slopes: evaluation of required reinforcement strength and embedment length using limit analysis. *Geotextiles and Geomembranes*, 44, p. 133-142.
- [28] Song F. Chen RY, Ma LQ & Cao G. (2016). A new method for the stability analysis of geosynthetic-reinforced slopes. *Journal Mountain Science* 13(11). DOI: 10.1007/s11629-016-4001-8
- [29] Christopher, B.R., Zornberg, JG, Mitchell, J.K. (1998). Design Guidance for reinforced soil structures with Marginal soil backfills. *Proc. of Sixth Int. Conf. on Geosynthetics, Atlanta, Georgia, March, Vol. 2, 797-804.*
- [30] Naughton, P.J., Jewell, R.A. & Kempton, G.T. (2001). The design of steep slopes constructed from cohesive fills and a geogrid. *Proc. of the International Symposium on Soil Reinforcement, IS Kyushu, Japan, p. 259-264.*
- [31] Clancy, J.M. & Naughton, P.J. (2008). Design of Reinforced soil structures using fine grained fill types. *Advances in Transportation Geotechnics - Ellis, Yu, McDowell, Dawson & Tom (eds.)*, Taylor & Francis, London, ISBN 978-0-415-475907
- [32] Giroud, J.P., Naughton, P.J., Rimoldi, P. & Scotto, M. (2014). Design of reinforced slopes and walls with low-permeability fills using draining geogrids. *Proc. of 10 Int. Conf. on Geosynthetics, Paper No. 248, September, Berlin Germany, 9 pages.*
- [33] Abd, A.H. and Utili, S. (2017). Design of geosynthetic reinforced slope

in cohesive backfills. *Geotextiles and Geomembranes*, 45, p. 627-641.

[34] Ingold, T.S.C. (1982). An Analytical study of Geotextile Reinforced Embankment. Proc. 2nd Int. conf. on Geotextiles, Las Vegas, IFAI, p. 683-688

[35] Leshchinsky, D. and Reinschmidt, A.J. (1985). Stability of membrane reinforced slopes. *J. Geotech. Engrg.*, 111(11), p. 1285-1300.

[36] Wright, S.G. and Duncan, J.M. (1991). Limit equilibrium stability analyses for reinforced slopes. Transportation Research Report, No. 1330, p. 40-46.

[37] Mandal, J.N. and Labhane, L. (1992). A procedure for the design and analysis of geosynthetic reinforced soil slopes. *Geotech. and Geological Engrg.*, 10(4), 291-319.

[38] Srbulov, M. (2001). Analysis of stability of geogrid reinforced steep slopes and retaining walls. *Computers and Geotechnics*, 28(4), p. 255-268.

[39] Shahgholi, M. & Fakher, A. and Jones, C.J.F.P. (2001). Horizontal slice method of analysis. *Geotechnique* 51(10), p. 881-885.

[40] Sawicki, A. and Lesniewska, D. (1989). Limit analysis of cohesive slopes reinforced with geotextiles. *Computers and Geotechnics*, 7, p. 53-66.

[41] Michalowski, R.L. and Zhao, A. (1993). Failure criteria for homogenized reinforced soils and application in limit analysis of slopes. Proceedings of Geosynthetics '93. Vancouver, Canada, p. 443-453.

[42] Michalowski, R.L. and Zhao, A. (1994). The effect of reinforcement length and distribution on safety of slopes. Proceedings of the 5th International Conference on

*Geotextiles, Geomembranes and Related Products*. Singapore, p. 495-498.

[43] Michalowski, R. L. and Zhao, A. (1995) Continuum versus structural approach to stability of reinforced soil structure. *J. of Geotechnical Engineering Division, ASCE*, 121, p. 152-162.

[44] Jiang, G.L. and Magnan, J.P. (1997). Stability analysis of embankments: comparison of limit analysis with method of slices. *Geotechnique*, 47(4), p. 857-872.

[45] Rowe, K. and Soderman, K. L. (1985). An approximate method for estimating the stability of geotextile-reinforced embankments. *Can. Geotechnical J.*, 22(3), p. 392-398.

[46] Almeida, M.S.S., Britto, A.M. and Parry, R.H.G. (1986). Numerical modeling of a centrifuged embankment on soft clay. *Can. Geotechnical J.*, 23, p. 103-114.

[47] Chalaturnyk, R.J., Scott, J.D., Chan, D.H.K. and Richards, E.A. (1990). Stresses and Deformations in a Reinforced Soil Slope. *Can. Geotechnical J.*, 28, p. 393-402.

[48] Ali, F.H. and Tee, H.E. (1990). Reinforced Slopes: field behavior and prediction. Proc. of the 4th Int. Conf. on Geotextiles, Geomembranes and Related Products, Hague, Netherlands, p. 17-20.

[49] Griffiths, D.V. and Lane, P.A. (1999). Slope stability analysis by finite element method. *Geotechnique*, 49, 3, p. 387-403.

[50] Krahn, J. (2003). The 2001 R.M. Hardy Lecture: The limits of limit equilibrium analyses. *Can. Geotech. J.*, 40, p. 643-660.

[51] Koerner, R. M. (1990). *Designing with Geosynthetics*, 2nd Ed., Englewood Cliffs, N.J. Prentice Hall

- [52] Fredlund, D.G., and Krahn, J. (1977). Comparison of slope stability methods of analysis. *Can. Geotechnical J.*, 14, p. 429-439.
- [53] Fredlund, D.G. (1984). Analytical methods for slope stability analysis. *Proc. of 4th Inter. Symposium on landslides, State-of-the-Art*, Sep. 16-21, Toronto, Canada, p. 229-250.
- [54] Reddy GVN, Madhav MR, Reddy ES (2008). Pseudo-static seismic analysis of reinforced soil wall effect of oblique displacement. *Geotextile & Geomembrane*, 26(5): p. 393-403.
- [55] Zornberg, J.G. and Mitchell, J.K. (1994). Reinforced soil structures with poorly draining backfills, Part I: Reinforcement Interactions and Functions. *Geosynth. Int.*, 2, p. 103-147.
- [56] Mitchell, J.K and Zornberg, J.G. (1995). Reinforced soil structures with poorly draining backfills Part II: Case Histories and Applications. *Geosynthetics International*, 2(1), p. 265-307.
- [57] Naughton, P.J., Giroud, J.P., Rimoldi, P., Scotto, M. and Crowther, D. (2015). The design of steep slopes using low-permeability fill and draining geogrids. *Proc. XVI ECSMGE*, ISBN 978-0-7277-6067-8
- [58] Giroud, J.P., 1983. Geotextile drainage layers for soil consolidation. *Civil Engineering for Practicing and Design Engineers*, Vol. II, p. 275-295.
- [59] Michalowski, R.L., 2013. Stability assessment of slopes with cracks using limit analysis. *Can. Geotechnical J.* 50 (10), p. 1011-1021.
- [60] Bishop, A. W. & Morgenstern, N. R. (1960). Stability coefficients for earth slopes. *Geotechnique*, 10, p. 129-150.
- [61] Jha A.K., Madhav Madhira and Reddy G.V.N. (2018). Analysis of Effect of Reinforcement on Stability of Slopes and Reinforcement Length optimization. *Geotechnical Engineering Journal of the SEAGS & AGSSEA*, Vol. 49 No. 4 December 2018 ISSN 0046-5828
- [62] Jha A.K., Madhira, M. and Reddy G.V.N. (2018). Mechanics of Reinforcement – Slope Interactions. *INAE Letters*, An official Journal of the Indian Academy of Engineering, ISSN 2366-326X, DOI 10.1007/s41403-018-0040-5
- [63] Jha A.K., Madhira, M. and Reddy G.V.N. (2016). Analysis of Effect of Reinforcement on stability of Slopes. *Indian Journal of Geosynthetics and Ground Improvement*, 2018, ISSN 2777-5633, 7, 1, p. 22-27.
- [64] Jha A.K., Madhira, M. and Reddy G.V.N. (2017). Analysis of Effect of Curtailment of Reinforcement on Stability of Steep Slopes. *Proc, 19<sup>th</sup> International Conference on Soil Mechanics and Geotechnical Engineering*, Seoul 2017, p. 2159-2162
- [65] Pockoski, M. and Duncan, J.M. (2000), "Comparison of Computer Programs for analysis of Reinforced slopes", Report of a study performed by the Virginia Tech Center for Geotechnical Practice and Research, Blacksburg, VA 24061.
- [66] Liu, C. N., K. H. Yang, Y. H. Ho, and Chang, C. M. (2012). Lessons learned from three failures on a high steep geogrid-reinforced slope. *Geotextiles and Geomembranes*, 34, p. 131-143.
- [67] Yang, K.-H., Thuo, J. N., Chen, J.-W. and Liu, C.-N. (2018). Failure investigation of a geosynthetic-reinforced soil slope subjected to rainfall. *Geosynthetics International*. [[https://doi.org/ 10.1680/jgein.18.00035](https://doi.org/10.1680/jgein.18.00035)].